Experimental methods of heavy-ion physics

V. L. Mikheev

Joint Institute for Nuclear Research, Dubna
Fiz. Elem. Chastits At. Yadra **10**, 269–313 (March–April 1979)

The main methods used to investigate nuclear reactions and products of reactions induced by heavy ions at energies up to ~10 MeV/nucleon are reviewed. Methods considered include the ΔE–E method, the time-of-flight method, magnetic analysis, and multiparameter measurements. The collection of recoil atoms and methods of identification of fusion products are described. A brief account is given of the Doppler-shift method and the blocking technique for measuring the lifetime of nuclear states. Some features of the operation of semiconductor detectors are analyzed and the possiblities of the photoemulsion method and solid-state track detectors for detecting heavy ions are considered.

PACS numbers: 25.70. – z, 29.30.Dn, 29.40.Pe

INTRODUCTION

Heavy-ion physics is the study of the mechanisms and products of nuclear reactions induced by ions of elements heavier than helium. Nuclear reactions on heavy ions with energies up to ~10 MeV/nucleon have been studied best. An ion energy of 10 MeV/nucleon ensures that the Coulomb barrier will be overcome in interactions with nuclei of all elements in the periodic table up to the very heaviest. Because of the difficulties of obtaining heavy-ion beams, investigations of nuclear reactions induced by them began much later than in the case of the lighter particles.[1,2]

At the present time, heavy-ion physics is a rapidly developing branch of science. To a large extent, this is due to the investigations made at the Laboratory of Nuclear Reactions at the Joint Institute for Nuclear Research at Dubna.[3,4] Let us at least mention here the main results: the synthesis of transuranic elements with atomic numbers Z from 102 to 107; the discoveries of fission isomers, emitters of delayed protons, and delayed fission of nuclei; and the discovery of deep inelastic nucleon transfer reactions. Reactions with heavy ions make it possible to study nuclei with maximally large angular momenta and to synthesize superheavy nuclei in the hypothetical new stability region ($Z \approx 114$).

The commissioning in recent years of new heavy-ion accelerators has made it possible to study nuclear reactions induced by ions of virtually all the elements up to uranium–uranium interactions.[5] The acceleration of heavy ions up to energies of order GeV/nucleon has opened up the field of relativstic nuclear physics.[6] For atomic physics, essentially new results have been obtained in the study of quasiatoms and quasimolecules[7] using beams of ions with energies ~1 MeV/nucleon, which do not exceed the Coulomb barrier. Study of the superheavy quasiatoms formed by the interaction of uranium with uranium makes it possible to verify the principles of quantum electrodynamics under conditions of superstrong electric fields.

The experimental methods of heavy-ion physics have been developed in an intimate interplay with those used for nuclear reactions on lighter particles at low, medium, and high energies. They are, however, distinguished by the greater number of products in the exit channels, the high ionizing capacity and, accordingly, short ranges of the particles, and the broad spectrum of charge states of the ions.

In this review, we concentrate our attention on the latest techniques used for heavy-ion beams with energies $\lesssim$10 MeV/nucleon. Various questions, especially those relating to the identification of reaction products, have already been covered in separate reviews.[8,9,10] Since the number of investigations in heavy-ion physics is continually increasing and the directions of investigations are becoming ever more particularized, it would be worthwhile to describe here, at least briefly, the methods that have already been most fully developed.

1. CHARACTERIZATION OF THE INTERACTIONS OF HEAVY IONS WITH NUCLEI

The main types of interaction of heavy ions with nuclei are shown schematically in Fig. 1. At the largest impact parameters and, accordingly, at the largest initial orbital angular momenta, elastic and inelastic scattering is predominant. The particle trajectories correspond basically to a purely Coulomb interaction.

At orbital angular momenta close to the value l_0 corresponding to a grazing interaction, there occurs not only scattering but also quasielastic transfer reactions involving a small number of nucleons. The value of this angular momentum can be determined from the relation

$$l_0 = 0.220\, R \sqrt{\mu\,(E_{\rm cms} - B_{\rm cms})},$$

where l_0 is the angular momentum measured in units of $\hbar$, R is the sum of the radii of the nuclei in units of

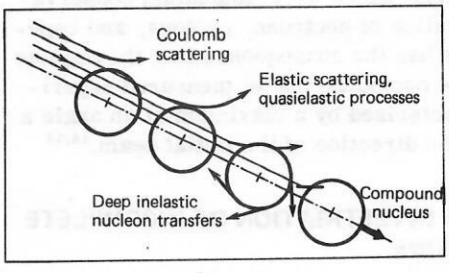

FIG. 1. Basic interactions of heavy ions with nuclei at different values of the impact parameter. The thick arrows reflect the typical directions of emission of the interaction products.

 0090-4759/79/020101-20$02.80

10^{-13} cm, E_{cms} and B_{cms} are the initial c.m.s. kinetic energy and the Coulomb barrier measured in MeV, and μ is the reduced mass in amu.

The angular distributions of the products for heavy target nuclei are characterized by maxima in the region of the angle θ_{cms} corresponding to Coulomb scattering in a grazing collision, in which the distance of closest approach of the nuclei is $R_{min}=R$. The angle θ_{cms} can be found from the relation

$$R=R_{min}=0.72\frac{Z_1Z_2}{E_{cms}}\left(1+\frac{1}{\sin\theta_{cms}/2}\right),$$

where Z_1 and Z_2 are the atomic numbers of the interacting nuclei. For light nuclei with mass numbers $A \lesssim 50$, for which the relative importance of the Coulomb interaction as compared with the nuclear reaction is considerably reduced, the angular distributions are characterized by a pronounced oscillatory structure.

On the transition from l_0 to the critical angular momentum below which the main process in the exit channel is the formation of a compound nucleus, the part played by deep inelastic nucleon transfers begins to increase. This process was first clearly revealed in experiments made at the Laboratory of Nuclear Reactions at Dubna[11,12] with the relatively light projectile particles ^{14}N, ^{22}Ne, and ^{40}Ar. Deep inelastic nucleon transfers make the main contribution to the total interaction cross section[13] in the case of the heavier particles ^{84}Kr and ^{136}Xe. The deep inelastic interaction is characterized by almost complete dissipation of the original kinetic energy, leading to the production in the exit channel of two products with energies corresponding to their exit Coulomb barriers. In deep inelastic interactions, tens of nucleons can be transferred from one nucleus to the other. Depending on the initial kinetic energy and the degree of rearrangement of the nuclei, the angular distributions of the products can vary from one peaked in the region of the angle θ_{cms} to distributions directed forward or even ones that are nearly isotropic. Many-particle processes are also observed in the same region of initial orbital angular momenta as the deep inelastic nucleon transfer. Their contribution to the total reaction cross section at $\lesssim$10 MeV/nucleon is smaller than that of the two-body processes.

At angular momenta smaller than the critical value, complete fusion of the original nuclei takes place. Without allowance for the de-excitation processes, the angular distributions of the compound nuclei are characterized by an accurate directionality along the original ion beam in accordance with momentum conservation. The evaporation of neutrons, protons, and especially α particles has the consequence that the angular distribution of the compound nuclei measured experimentally is characterized by a maximum at an angle a few degrees off the direction of the initial beam.[14,15]

2. METHODS OF INVESTIGATION OF INCOMPLETE FUSION REACTIONS

In the general case, the experimental methods of investigation of the mechanisms and products of nuclear reactions with heavy ions reduce to Z and A identification of the products in the exist channel, the determination of their energy states and lifetimes, and the measurement of the angular and energy distributions as a function of the energy and species of projectile and target.

Somewhat arbitrarily, the methods of investigation of heavy-ion reactions can be divided into the methods of investigation of incomplete fusion reactions and investigation of complete fusion reactions. Of course, a clear demarcation of these methods does not exist. To some extent, they are characterized by differences in the angular distributions (see Fig. 1). As a result, the products of incomplete fusion reactions are separated from the beam simply because they are emitted in directions that do not coincide with the direction of the beam. It is therefore easy to investigate the products of the nuclear reactions in flight after they have left the target on account of the projectile momentum.

$\Delta E - E$ Method

Wide use of the $\Delta E-E$ method in heavy-ion physics was initiated by the pioneering work of Ref. 16. The Bethe–Bloch equation for the specific energy loss of a heavy charged particle has in the general case the form[8]

$$-\frac{dE}{dx}=4\pi n\frac{e^4q_{eff}^2}{mv^2}\left\{\ln\left[\frac{2mv^2}{I(1-\beta^2)}\right]-\beta^2-S-D\right\},$$

where n is the number of electrons in 1 cm^3 of the absorber, e and m are the charge and mass of the electron, q_{eff} is the effective charge of the ion in units of the electron charge, v is the ion velocity, β is the ratio of v to the velocity of light, I is the mean ionization potential of the absorber, S is a shell correction, and D is a density correction.

Ignoring the energy dependence of the logarithmic term, we readily obtain $EdE \sim E\Delta E \sim Aq_{eff}^2 \sim AZ^2$, where A is the mass number of the detected particle; the transition from dE to ΔE reflects the finite value of the energy loss in a real absorber, whose part is played by the ΔE detector. Thus, by measuring the two parameters E and ΔE one can obtain the value of Aq_{eff}^2. The value of q_{eff} satisfies $q_{eff} \leq Z$ and depends on Z, the ion velocity, and the stopping medium. In real measurements, q_{eff} is discrete because Z is. In practice, one can always perform a calibration on the elastically scattered initial particles with known Z and A; furthermore, the Z and A of the products form a sequence of integer numbers. Therefore, in $\Delta E-E$ two-parameter measurements one can reliably identify the detected events. Part of the two-dimensional $\Delta E-E$ spectrum obtained from the bombardment of ^{232}Th by 174-MeV ^{22}Ne ions using a telescope of silicon detectors in experiments made at the Laboratory of Nuclear Reactions[11] is shown in Fig. 2. There is no doubt that the elements have been reliably identified. In these experiments, no attempt was made to distinguish individual isotopes.

As a rule, one uses as parameter of identification PI, not the directly measured $E\Delta E$, but certain other combinations of E and ΔE that make it possible to eliminate the energy dependence of PI:

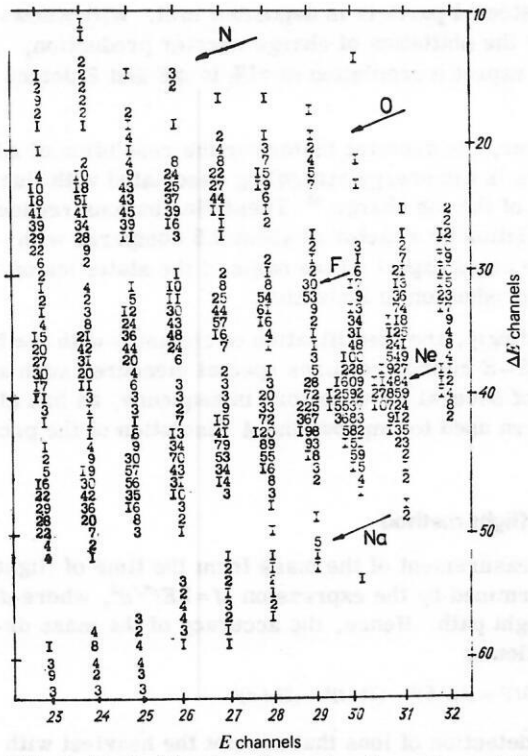

FIG. 2. Part of the two-dimensional spectrum obtained at angle 40° to the beam resulting from bombardment of ^{232}Th by 174-MeV ^{22}Ne ions. A telescope of silicon detectors. Detector thickness $\Delta E = 27$ μm.

1) $PI = \Delta E(E + a\Delta E + b)$, where a and b are experimentally chosen parameters. An example is provided by the data in Fig. 3, which is taken from Ref. 17.

2) $PI = \Delta x/a = [(E + \Delta E)^n - E^n]$. This expression is obtained on the basis of the empirical energy dependence $R = aE^n$ of the range, in which a is a constant that depends on the particle species; $n = 1.73$ for a wide range of particles and energies[18]; Δx is the thickness of the ΔE detector. The further development of this approach in Ref. 19 led to the expression $PI = \{[(E + \Delta E)/K]^n - (E/K)^n\}^{1/2}$, where $n = b - c\Delta E/(\Delta x E)$, and b and c are constants chosen experimentally to make PI as independent of E as possible; K is a normalization constant associated with the number of channels in the detecting electronics.

Rather than approximating the range–energy curves by analytic dependences, some experimenters have used the experimental range–energy relation $R = f(E)$, which is fed into a computer and used to identify the particles.[20]

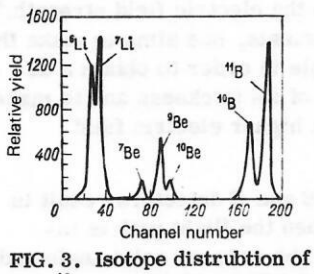

FIG. 3. Isotope distrubtion of products of interaction of ^{11}B with ^{12}C at 115.5 MeV. The ΔE detector is an ionization chamber; the identification parameter is $\Delta E(E + a\Delta E + b)$.

3) $PI = \Delta E + KE$. This expression was used, for example, in Ref. 21. It presupposes a linear dependence of the type $\Delta E = E_0 - KE$ in the two-dimensional spectra, K being an experimentally chosen constant that depends on Δx. This relation is convenient for detection of products in relatively narrow energy intervals. The expressions we have given by no means exhaust all possible variants of expressions that can be used as PI, but they are the ones most widely used.

ΔE Detectors. Thin plane-parallel silicon surface barrier ΔE detectors and gas ionization chambers are widely used as ΔE detectors. Typical thicknesses of the silicon detectors are 10–100 μm. According to the data published in Ref. 22, the most sensitive surface for detectors with thickness ~60 μm is 3 cm^2. The sensitive surface of detectors <10 μm thick does not as a rule exceed a few tens of mm^2. Thus, according to the published data[23], the thinnest (1.7 μm) known ΔE detector has a sensitive surface 7 mm^2. As the thickness of the detectors is reduced, their relative inhomogeneity increases strongly, and there is a sharp deterioration of the energy resolution. For example, the 1.7-μm thick ΔE detector had a relative inhomogeneity of ~20%. The best result obtained for silicon detectors is an energy resolution of 3% for a 3.8-μm thick detector and ^{40}Ar ions; this is virtually the same as the best results obtained with much thicker detectors.[24]

The acceleration of ever heavier ions such as Kr and Xe has made it necessary to develop ΔE detectors that satisfy a number of rather stringent conditions. For operation with the heaviest ions, the effective thickness of the detector must not exceed ~10 μm silicon equivalent because of the high specific energy losses of the detected particles. The energy resolution must distinguish elements up to $Z \approx 50$. The requirement of a high detection efficiency makes it necessary to have a sensitive surface ≥1 cm^2.

To a considerable extent, all these requirements are met by specially developed gas ionization chambers. Typical constructions of ionization chambers of ΔE type developed in recent years are described in Refs. 25–28. As a rule, the effective thickness of the working gas in them is equivalent to a few microns of silicon. The entrance window, which isolates the gas from the vacuum chamber of the accelerator, can be made fairly thin. For example, a 16-μg/cm^2 parylen C film was used in Ref. 26 as entrance window. On a supporting mesh with 97% transparency and window measuring 10 × 25 mm^2, this film withstood pressures up to 40 Torr. The residual energy E of the particles is measured by a semiconductor detector directly in the working gas that forms the rear boundary of the gas volume through which the detected particles pass.

The development of ionization chambers with maximally high Z resolution showed that it is better to use a pure methane filling rather than the widely used gas mixture of 90% argon and 10% methane. According to the data of Ref. 29, the resulting relative improvement in the energy resolution is about 20%. In Ref. 29, 180-

MeV ^{129}Xe ions were detected by a ΔE ionization chamber with methane filling, and a resolution $\Delta Z/Z = 0.9/54$ (FWHM) with respect to the atomic number was obtained. The particles lost 30% of their initial energy in the ΔE detector.

The improved resolution for the detection of heavy ions in ionization chambers with pure methane filler can be attributed to the use of much higher voltages on the electrodes than for the argon + methane mixture.[30] The greater intensity of the electric field reduced the recombination of the charge carriers in the track of a heavily ionizing particle.

Ultimate Capabilities of the ΔE–E Method. In the ΔE–E method, all identification parameters are ultimately proportional to the product $P = AZ^2$. Therefore, the limits of resolution with respect to Z are twice those with respect to A:

$$\frac{dP}{dA}\frac{1}{P} = \frac{1}{A}; \quad \frac{dP}{dZ}\frac{1}{P} = \frac{2}{Z}.$$

Accordingly, the best results in the $\Delta E - E$ method hitherto have involved A resolution up to $A = 21$ (oxygen isotopes) and atomic number resolution up to $Z \approx 60$. These were obtained in Refs. 31 and 32, results of which are shown in Fig. 4. A single ΔE detector was already insufficient for distinguishing the oxygen isotopes, and a telescope with two ΔE detectors was employed. By comparing the pulse amplitudes when two detectors are used, one can improve the peak–dip ratio in the amplitude spectra by discrimination of events that give pulses of reduced amplitude in one of the detectors because of channeling and incomplete collection of the charge carriers. To extend the identification to higher A, it is advisable to use the time-of-flight technique.

As regards Z identification of the products of nuclear reactions, the ΔE–E method is still the one most widely used. However, to distinguish individual elements in the region $Z \gtrsim 50$ it is necessary to use special mathematical methods to evaluate the raw two-dimensional spectra.[32]

The limits of the Z and A resolution in the ΔE–E method are determined by the energy resolution of the ΔE and E detectors. To achieve the best energy resolution in both detectors, the thickness of the ΔE detector is chosen such that approximately half of the energy

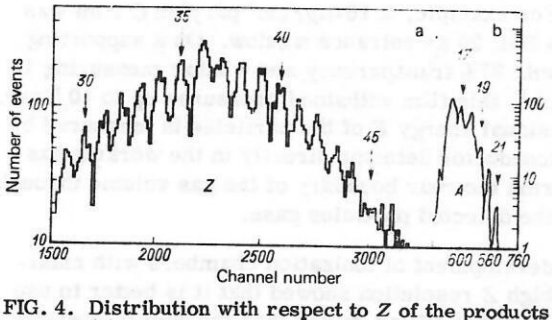

FIG. 4. Distribution with respect to Z of the products of the reaction ^{159}Tb + ^{86}Kr (620 MeV) obtained at the angle 20° by means of a telescope consisting of a ΔE ionization chamber and silicon detector[31] (*a*), and A separation of oxygen isotopes obtained from the interaction ^{197}Au + p (3 GeV) (*b*) (Ref. 30).

of the detected particle is deposited in it. With allowance for the statistics of charge carrier production, one can expect a resolution of ~1% in ΔE and E detectors.[33]

However, the decisive factor for the resolution of ΔE detectors is the energy straggling associated with fluctuations of the ion charge.[34] These fluctuations reduce the resolution by a factor of about 2.5 compared with what one could expect on the basis of the statistics of carrier production in ionization.

Accordingly, the identification of elements with $Z \gtrsim 50$ in the ΔE–E method requires special measures such as the use of several ΔE detectors in sequence, as has already been used to improve the A resolution of the products.

Time-of-flight method

The measurement of the mass from the time of flight t is determined by the expression $M = 2Et^2/d^2$, where d is the flight path. Hence, the accuracy of the mass determination is

$$(\delta M/M)^2 = (\delta E/E)^2 + (2\delta t/t)^2 + (2\delta d/d)^2.$$

For the detection of ions that are not the heaviest with $\delta E/E \lesssim 1\%$ the value of $\delta d/d$ is negligibly small. Therefore, the main factor determining $\delta M/M$ is the time resolution $\delta t/t$.

The velocity of heavy ions is determined by the expression $v = 1.389\sqrt{E/M}$ cm/nsec with E measured in MeV and M in amu. At the typical energy 5 MeV/nucleon, we obtain a time of flight of 33 nsec over a flight path of 100 cm. Accordingly, if we wish to resolve masses around $M \approx 50$, we must have a time resolution of ~0.3 nsec.

Measurement of the Time of Flight between Silicon Detectors. It is very natural to augment the ΔE–E method by measuring the time of flight of particles between detectors separated by several tens of centimeters.

In Ref. 23, in which ΔE detectors of thickness 1.7–17 μm and E detectors of thickness 170 μm were used, a time resolution of 0.1–0.4 nsec was achieved. The detectors were cooled to between −20 and −50 °C. Cooling the detectors increases the carrier mobility, reduces the leakage currents, and makes it possible to use a higher bias voltage. An increased electric field intensity in the detector reduces the time of spreading of the plasma in the tracks of heavily ionizing particles, which is inversely proportional to the electric field strength.[35] For time-of-flight measurements, one aims to make the E detector as thin as possible in order to obtain a depleted layer over the whole of its thickness and to make it possible to operate with a higher electric field strength.

The restricted sizes of ΔE and E detectors result in serious efficiency losses when the flight path is increased, on account of both the reduced solid angle and multiple scattering in the ΔE detector. The rms angle of multiple scattering can be estimated[8] in accordance

with the relation

$$\theta = 1.8\left\{\frac{3.922\cdot 10^{-8}\Delta x Z_1 (Z_1+1) q_{\text{eff}}^2}{A_1 E^2}\ln\left[\frac{208.1\Delta x}{(Z_1^{2/3}+q_{\text{eff}}^{2/3})}\frac{Z_1+1}{A_1 Z_1}\right]\right\}^{1/2},$$

where A_1 and Z_1 refer to the scattering material of thickness Δx μg/cm^2, and E is measured in MeV.

According to the estimates of Ref. 23, multiple scattering in a 1.7-μm thick ΔE detector of area 7 mm^2 has the consequence that about 40% of the fragments of ^{252}Cf fission that pass through the ΔE detector exactly along the line joining the centers of the ΔE and E detectors do not hit an E detector of area 200 mm^2 at a distance of 50 cm.

The limitations on the detection efficiency and the not always available possibility of combining in one detector the functions of amplitude and time measurement have led to the use of special devices rather than ΔE detectors to measure the zero time.

Thin Scintilation Films. Numerous plastic scintillators with de-excitation times of ~1 nsec can be obtained[36] in the form of films thinner than 1 μm and still give a light yield sufficient for a time resolution better than 1 nsec in the detection of heavy ions. Typical detectors of this kind are described in Refs. 37–39. A serious problem here is the guiding of the relatively small number of photons from the scintillator to the photomultiplier cathode. Usually, one either fixes the films between halves of a light pipe with an opening for the particle beam,[37] or one uses a hemispherical mirror that collects the light onto the photocathode.[38,39] Films of the necessary thickness can be prepared relatively easily directly in the laboratory.[39] To choose the necessary thickness of the film, one can use the result of Ref. 39 that the optimal film thickness, above which the time resolution is not improved, corresponds to energy losses ~600 keV.

A time resolution of about 0.3 nsec has been achieved[38,39] in real systems using telescopes with a thin film to give the starting time signal and silicon detectors to give the stop signal.

Emission of Electrons from Thin Foils. The emission of electrons from thin foils when heavy ions pass through them is finding ever wider use in time-of-flight measurements. The energy spectrum of these electrons is almost entirely concentrated in the range up to 10 eV.[40,41] According to the data of Ref. 41, the most probable energy of secondary electrons from a 25-μg/cm^2 thick aluminum foil is ~1.8 eV for α particles and ~0.3 eV for fission fragments.

The yields of secondary electrons are well correlated with the specific ionization energy losses of the particles.[42] If sufficiently thin foils (6 μg/cm^2 carbon) are used, the yield from two foils is more than twice the yield of electrons from one foil. This is due to multiplication of relatively more energetic electrons.

Experimental data[42] on the number of secondary electrons produced in carbon films by various ions are given in Fig. 5. The number of secondary electrons emitted by a 6-μg/cm^2 carbon foil is already about 100

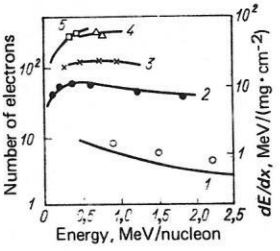

FIG. 5. Yield of secondary electrons as a function of the atomic number and energy of heavy ions. 1) He(Z=2), 2) O(Z=8), 3) S(Z=16), 4) Tc(Z=43), 5) Cs(Z=55). The yield numbers were obtained by subtracting the effect from one carbon foil of thickness 6 μg/cm^2 from the effect of two foils. The curves are calculations of the specific ionization in accordance with Ref. 69 normalized to the yield of electrons for sulfur.

at Z=16. A system of several foils can be used to determine the Z of a particle on the basis of the number of secondary electrons with an accuracy that approaches that of ΔE detectors.

When secondary electrons are used for time measurements, it is important to ensure that the electrons move isochronously from the region in which they are produced to the detection region. This is achieved by increasing the velocity of the electrons by accelerating them to 1–10 keV, and also by careful choice of the geometry of the electric and magnetic fields in which the electrons move. To detect the secondary electrons in timing measurements, one uses scintillation and silicon detectors, open electron multipliers, channel electron multipliers, and microchannel plates.

In Ref. 43, the zero time detector was a 0.5-μm aluminum foil at a potential of 20 kV. The secondary electrons from the foil were detected by two scintillation counters in coincidence. The stop signal was given by a silicon detector. A time resolution of ~2 nsec was achieved.

In Ref. 44, a time resolution ~0.3 nsec was obtained with detection by a silicon surface barrier detector of secondary electrons accelerated to 18–24 keV. If devices are used that multiply directly the electrons that enter them, it is sufficient to accelerate the electrons from the foil to about 1 keV. A time resolution ~1 nsec was achieved[45] by means of an open electron multiplier, and ~0.35 nsec was achieved[46] by means of a channel electron multiplier.

The best devices for detecting secondary electrons appear to be microchannel plates.[47,48] Their use in Ref. 49 resulted in a time resolution of 0.08 nsec for 100-MeV ^{16}O ions. The arrangement of them for detecting secondary electrons is shown in Fig. 6.

Because of the relative novelty of these devices, we give a brief description of them. The microchannel plate is prepared by cutting a plate of thickness ~1 mm from a packet of glass capillaries of internal diameter 10-50 μm welded together. The diameter of the complete packet may reach 50 mm. The surface of an ordinary microchannel plate is perpendicular to the axis of the capillaries. The plate is then exposed in a chemically active atmosphere to make the walls of the capillaries

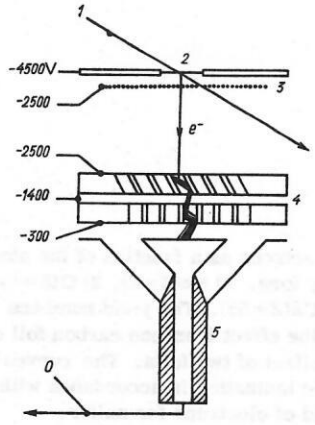

FIG. 6. Detection of secondary electrons by means of chevron microchannel plates. 1) Particle; 2) thin foil; 3) accelerating grid; 4) microchannel plates; 5) coaxial anode.

conducting (10^{10}–10^{12} Ω/channel). When a voltage ~1 kV is applied, the slightly conducting surface of the channel walls forms a continuous amplifying divided dynode system with amplification 10^3–10^4. The directly measured signal is taken from a coaxial grounded anode, which the multiplied electrons strike after they have left the channels.

The multiplication obtained with a single plate is restricted by the parasitic emission of positive ions. These ions are produced by ionization by the electrons of the residual gas at the exit end of the channel. After they have been formed, the ions are accelerated to the entrance end of the channel, where they knock electrons out of the walls. The electrons are then accelerated in the usual manner and the plate is saturated. The problem of the background of positive ions was solved by the so-called chevron microchannel plates.

These are made as composites together with an ordinary plate and are cut at an angle ~15° to the axis of the capillaries. The positive ions produced at the exit of the ordinary plate move, in contrast to the electrons, along a straight line and cannot reach the entrance of a plate cut at an angle. Both plates work with a multiplication of 10^3–10^4. The electrons from the positive ions are multiplied in one plate, and the electrons from the working signal are multiplied in both plates. This is sufficient to suppress the background.

Parallel Plate Avalanche Counters. These have been introduced in recent years in heavy-ion physics for timing measurements[50]; they usually consist of two thin plastic metallized films fixed parallel to each other and separated by 1–3 mm. A potential difference of a few hundred volts is applied between the films. The ionizing particles pass through the counter approximately perpendicularly to the surface of the films and produce electron–ion pairs in the working gas between the films. A Townsend avalanche develops in the strong homogeneous electric field. The number of secondary electrons is

$$n(d) = n_0 \exp(\alpha d),$$

where n_0 is the number of primary electrons, d is the drift path, and α is the first Townsend coefficient. The coefficient α is the mean probability of ionization per unit path length and is a function of the reduced electric field strength:

$$\alpha/P = C\exp[-B/(E/P)],$$

where P is the gas pressure, and C and B are constants for a given gas. At $E/P \approx 500$ V·cm^{-1}·torr^{-1}, it is possible to obtain a gas multiplication ~10^4. Methylal, isobutane, isobutylene, pentane, heptane, and mixtures of these gases have proved to be good working gases. The optimal range of pressures is 8–15 torr. At lower pressures, the original ionization is too weak, and at higher pressures there are problems with the films that separate the region containing the parallel plate avalanche counters from the vacuum. The typical amplitude of a signal is a few millivolts. The signal can be divided into two parts: a fast electron component (rise time ~2 nsec) and a slow component from the positive ions (rise time ~1 μsec).

In Ref. 50, a time resolution of 0.16 nsec (FWHM) was achieved in the detection of 25-MeV ^{16}O ions by means of a parallel plate avalanche counter of area 50 cm^2.

Because of the relatively low absorption of energy in them, industrially produced films of thickness 2–3 μm make it possible to use two successive avalanche counters of this kind to give the start and stop signals in time-of-flight measurements.

The working area of such a counter can be increased to 1 m^2 by subdividing it into several sections, the signal from each of them being detected separately.[51,52] This makes it possible to use large solid angles and to investigate many-particle processes.

Double Measurement of the Time of Flight. A use of the time-of-flight method that warrants notice was found in Ref. 53. Here, there was a double measurement of the time of flight—before the energy absorber and after it. This made it possible to determine the energy loss in the absorber from the time of flight and therefore to obtain data for determining Z from time rather than amplitude measurements.

Magnetic analysis in conjunction with the $\Delta E - E$ and time-of-flight methods

The use of magnetic spectrometers to investigate the mechanisms and products of reactions induced by heavy ions has a number of advantages over simple detector telescopes. In the first place, there is the possibility of exploiting the difference in magnetic rigidity to separate spatially the elastic scattering peak and the products of nuclear reactions. The focusing properties of magnetic spectrometers make it possible to use large solid angles over flight paths of several meters. The highest accuracy in the measurement of the energy spectra is also ensured by magnetic spectrometers.

The first models of magnetic spectrometers[54,55] used in experiments with heavy-ion beams made it possible to obtain very valuable scientific information, although their construction was inadequate to take into account the specific features of work with heavy ions. The ex-

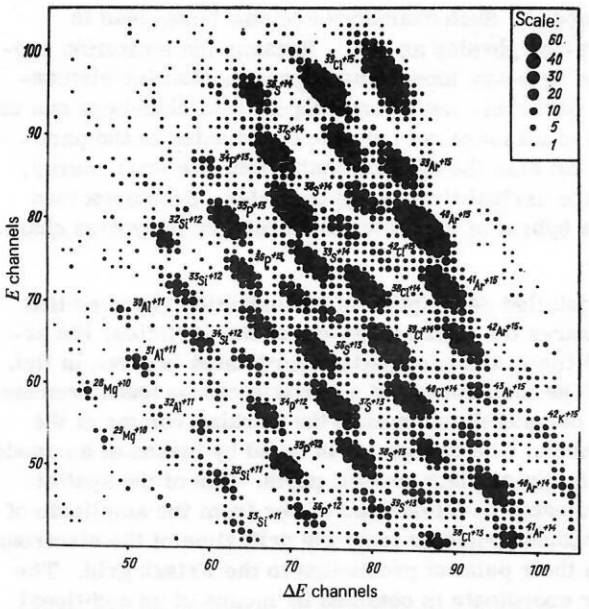

FIG. 7. Two-dimensional spectrum obtained by bombarding ^{232}Th with 290-MeV ^{40}Ar ions. A telescope of silicon detectors was placed at the exit focus of the magnetic spectrometer. Thickness of the detector $\Delta E = 36$ μm.

periments of Ref. 55 used a magnetic spectrometer with homogeneous field and double focusing of second order; it was a copy of a spectrometer constructed to study scattering of electrons with momenta up to 400 MeV/c.[56] It has the following main parameters:

radius of central trajectory	1.26 m
deflection angle	70°
maximal field	1.8 T
solid angle	$3 \cdot 10^{-3}$ sr
momentum dispersion	12.7 mm/1%
momentum resolution with source of diameter 10 mm	0.3%

Using a telescope of silicon detectors placed at the exit focus of the spectrometer, one can establish the atomic number of particles up to $Z \approx 20$ and the mass number up to $A \approx 50$.

The two-dimensional ΔE–E spectrum obtained with a telescope at the exit focus of the magnetic spectrometer is shown in Fig. 7 for bombardment of ^{232}Th by 290-MeV ^{40}Ar ions.[57] Each group of events revealed by the clustering of the circles corresponds to an individual isotope in a definite charge state.

A significant extension of the possibilities of a ΔE–E telescope is due to the fact that when particles of a definite magnetic rigidity are separated by means of the magnetic spectrometer the relative change in the amplitudes of the pulses in the ΔE and the E detectors when A changes is much larger than without preliminary magnetic analysis:

$$d(\Delta E)/\Delta E = 2dA/A; \quad dE/E = -\frac{(E_0/\Delta E)+2}{(E_0/\Delta E)-1}\frac{dA}{A},$$

where $E_0 = E + \Delta E$.

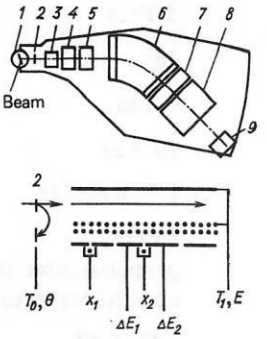

FIG. 8. Magnetic spectrometer used with the heavy-ion accelerator at Darmstadt. 1) Target; 2) zero-time detector; 3) and 7) sextupole magnets; 4), 5), and 8), quadrupole magnets; 6) dipole magnet; 9) focal gas detector, shown in the lower part of the figure.

The magnetic spectrometers constructed in recent years have taken into account a number of features of work with heavy ions. Above all, because of the broad spectrum of the products of nuclear reactions with respect to Z, Z_i, A, and E, the detecting device of the spectrometer must have a complicated structure, making possible the measurement of ΔE, E, the time of flight, and the coordinates of the particles.

In spectrometers designed for work with electrons and protons, frequent use was made of detection by photographic plates placed in the focal plane. It was convenient to have the focal plane at an angle ~45° to the central trajectory. For modern multiparameter detecting devices it is much more convenient to have the focal plane perpendicular to the central trajectory.

For time-of-flight measurements, it is necessary to ensure that the particles move as isochronously as possible in the spectrometer, since otherwise it is necessary to adopt special measures to compensate for the spread of the path lengths. This was achieved, for example, in Ref. 58 by the development of a start-time detector in the form of a thin scintillation film placed at an angle of 15° to the central trajectory.

For work with beams of heavy ions whose masses are comparable with that of the target nucleus, it is very important to compensate for the kinematic change in the energy of the reaction products as a function of the angle within the acceptance angle. According to the data of Ref. 59, the kinematic change in the energy for acceptance angle $\Delta\theta = 6.5°$ is ~13% for elastic scattering of equal-mass particles through 30°, which is hundreds of times greater than the energy resolution of modern spectrometers. All these requirements can be met only in an already complicated magnetic system, which consists of several elements, including dipole and quadrupole and more complicated magnets to guarantee kinematic compensation.[59]

The most modern type of magnetic spectrometer for heavy ions is probably the spectrometer (Fig. 8) developed for the heavy-ion accelerator at Darmstadt in West Germany.[10,28] The main parameters of the spectrometer are as follows:

magnetic rigidity	3 T·m
deflection angle	45°
total length	7.5 m
solid angle	10^{-3} sr
dispersion	1.5–6 cm/1%
focal plane	50 cm; perpendicular to central trajectory
energy acceptance	±33–8.5%
energy resolution	5×10^{-4} without kinematic compensation; 10^{-3} with kinematic compensation
difference of path lengths	6×10^{-3}
detection angles	from −135° to +135°
total mass of magnetic systems	30 ton
mass of platform	7 ton

The system for detecting the reaction products in the focal plane is a further development of the similar systems using magnetic spectrometers at Berkeley[60] and Rochester.[61] The detector has an entrance window measuring 50 × 6 cm in the focal plane. It is an ionization chamber with a large number of electrodes to make possible the measurement of many parameters.

The anode of the chamber is cut into parts, each of which can be used to measure the specific ionization ΔE. Behind the slits that separate the parts of the anode there are proportional counters, whose wires have a high resistance. The electrons produced by the heavy particles drift toward these counters along the lines of force of the homogeneous electric field and pass through the slits into the sensitive region of the counters. By measuring the rise time[62] or by measuring the ratio of the currents at opposite ends of the wire[63] one can determine the position at which the particle passed with an accuracy of ~1 mm. The signals corresponding to the total energy of the particle and the time of arrival of the particle in the focal plane are taken from the cathode, which is connected to the first grid through a capacitance. The start signal is taken from the detector of the secondary electrons, which is situated at the entrance to the spectrometer. It can be constructed in such a way as to give information about the position at which the heavy particle passes and, accordingly, the exact angle of entrance into the spectrometer within the acceptance angle.[64]

Ionization detectors with measurement by the $\Delta E-E$, time-of-flight, and particle-coordinate methods

Recent years have seen the every wider application of gas ionization detectors in the study of nuclear reactions. In high-energy physics, the most characteristic apparatus of this kind is the multiwire proportional chamber.[65] Such chambers are now being used in heavy-ion physics as well. Because the ionization produced by heavy ions is much greater than for elementary particles, multiwire proportional chambers can be used to measure not only the coordinates of the particles but also the specific ionization, the total energy, and the arrival time of the particles. Such detectors are a hybrid of multiwire and ordinary ionization chambers.

A detailed description of an ionization chamber that measures the total energy ΔE of the particles, the arrival time, and two spatial coordinates is given in Ref. 66. The total energy of a particle can be found because it is completely stopped in the working volume of the chamber. The energy ΔE is found by means of an anode that is divided into several parts. One of the spatial coordinates is determined either from the amplitude of the cathode pulse or from the drift time of the electrons from their point of production to the Frisch grid. The other coordinate is obtained by means of an additional multiwire grid placed between the Frisch grid and the anode. The individual wires of the additional grid are connected to resistances, which makes it possible to use the charge division method to determine the coordinate. The time signal is taken from the cathode. The rise time of the signals in the ionization chamber is long (~1 μsec), but with a large signal-to-noise ratio, which is characteristic for heavy ions of ~100 MeV, a time resolution <1 nsec is fully attainable.

A detector closest in type to the multiwire chambers of high-energy physics is used in the many-particle coincidence spectrometer on the heavy-ion accelerator at Darmstadt.[51,52] The spectrometer is a scattering chamber with a diameter of about 3 m and height about 2.7 m in which two detectors, each with a sensitive surface ~1 m^2, can be moved independently through the angles. The schematic arrangement of one of the detector variants is shown in Fig. 9. It is an aluminum frame with a Hostaphan vacuum entrance window of thickness 2.5 μm (330 $\mu g/cm^2$) cut out of a complete strip 1.5 m wide. The window is spanned over supporting wires 200 μm thick at every 15 mm. Five grids are

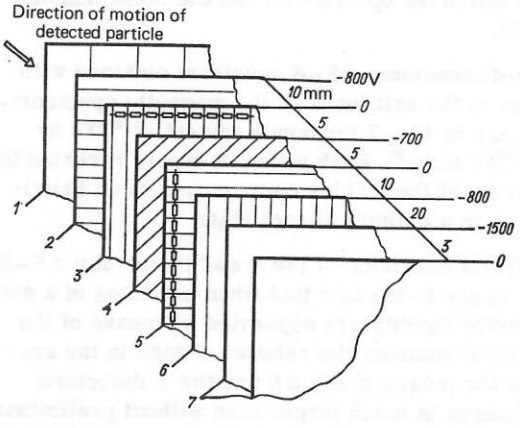

FIG. 9. Ionization detector with area 1 m^2 for measuring two coordinates, the specific ionization, and the time of flight. 1) Entrance window, 2) and 6) cathodes, 3) multiwire detector for x, 4) anode, 5) multiwire detector for y, and 7) electrodes of the parallel plate avalanche counter.

arranged over the total thickness of the detector (about 5 cm). Each grid consists of CuBe wires 50 μm thick every 2 mm. Two of these grids, with mutually perpendicular wires, are used to determine the x and y coordinates. The wires in the grids are connected to each other through a 100-Ω resistance. Information is read out by the current division method by means of amplifiers connected to the wires every 80 mm (12 amplifiers for 500 wires in one plane). The total current from the signal planes is a measure of the specific ionization ΔE of the particle. Two other grids are used as cathodes, and one—with diagonal arrangement of the wires—as anode. A parallel plate avalanche counter forms the rear part of the detector. The entrance electrode is a well spanned film of Hostaphan 2.5 μm thick, onto which a layer of gold has been deposited by vacuum evaporation. The second electrode is a sheet of Plexiglas, onto which gold has also been deposited. The distance between the electrodes of the parallel plate avalanche counter is 3 mm. Because it is hard to maintain a constant gap between the electrodes of the parallel plate avalanche counter, it is made in the form of nine individual identical detectors, each with a working area ~0.3 × 0.3 m. In turn, the gold layer on the Plexiglas in each of the detectors is deposited in the form of strips of a few centimeters width, these being electrically insulated from one another. The signal is read off from each of the strips independently. This makes it possible to increase the amplitude and improve the time properties of the signals from the parallel plate avalanche counter. In addition, this arrangement in sections of the parallel plate avalanche counter together with the sectioned readout of information from the x and y planes makes it possible to establish the simultaneous production of several particles in a single nuclear interaction. One of the working gases that is used is isobutylene at a pressure 5–10 torr.

A time resolution of ~0.5 nsec and a 10% resolution in the measurement of the specific energy losses were achieved in experiments with a Kr beam. The accuracy in the measurement of the coordinates was <3 mm. In the detector variant with determination of the coordinates by measurement of the delay time of the signal from individual wires, a spatial resolution ~0.5 mm (FWHM) was achieved. In the existing variant of the detector, the total energy of the particles is not measured, although this is in principle possible.

3. METHODS OF INVESTIGATION OF COMPLETE FUSION REACTIONS

As we have already noted, the compound nuclei formed in complete fusion reactions leave the target along a direction that virtually coincides with the direction of the beam. When one is working with intense beams, it is particularly important to separate the products of the interactions from the region of the ion beam. Here and in what follows, we shall be considering products with lifetimes $\lesssim$1 min, for which the usual radiochemical methods of separation from bombarded samples are not sufficiently fast.

In the study of the reactions and products of complete fusion, the most effective method is to exploit a characteristic of the heavy ions such as the large momenta transferred to the interaction products. A target ~1 mg/cm^2 thick, which is self-supporting or desposited on a substrate, is exposed to a beam of heavy ions. Because of the momentum of the projectiles, the recoil atoms are knocked out of the target. This solves the problem of separating the virtually single new atoms from the 10^{18}–10^{19} atoms of the target. Here and in what follows, we shall use the expression *recoil atoms*, but it must be borne in mind that the reaction products are knocked out of the target in the form of ions with fairly high charges. The problem of separating the recoil atoms and the products of their decay from the region of the beam can be solved in different ways.

For products with half-life $\geq 10^{-4}$ sec there are three main groups of methods for transferrring the radioactive atoms from the region of the beam to detectors of radioactive decay: 1) purely mechanical methods in which the recoil atoms strike into the surface of a rotating disk or moving band, which carry the products to the radiation detector; 2) transport of the recoil atoms by gas flows; 3) separation of the recoil atoms from the ion beam by means of electric and magnetic fields. The last method makes it possible to study nuclei with lifetimes down to 10^{-7} sec. The decay of nuclei with lifetimes 10^{-7}–10^{-12} sec can be detected in flight after they leave the target. For this one uses the noncoincidence between the angles of emission of the decay products and the direction of the beam.

Lifetimes of compound nuclei in the range 10^{-16}–10^{-19} sec can be measured by bombarding targets in the form of single crystals; in this case the nuclei decay while traversing interatomic distances.

Irrespective of the lifetimes, complete fusion processes can be studied through the kinematics of the decay processes of the compound nuclei.

Mechanical Methods of Transporting Recoil Atoms. An advantage of the mechanical methods of transport is the simplicity and 100% efficiency of collection of the recoil atoms knocked out of the target. In the study of processes with the smallest cross sections studied in heavy-ion physics (10^{-35} cm^2), these are the most efficient methods.

Figure 10 shows the schematic arrangement of an experiment[67] on the synthesis of a spontaneously fissioning isotope of the 104-th element ^{260}Ku with half-life 0.1 sec

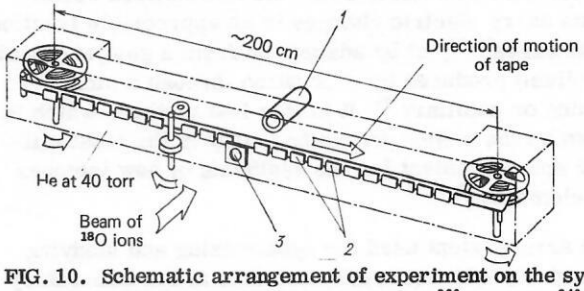

FIG. 10. Schematic arrangement of experiment on the synthesis of the spontaneously fissioning isotope ^{260}Ku in the ^{246}Cm(^{18}O, 4n) reaction. Helium is used to cool the target and the tape collector.

produced by bombardment of ^{246}Cm ions with ^{18}O. The recoil atoms are collected by a nickel tape 10–20 μm thick, 25 mm wide, and up to 800 m long. It is wound at a speed up to 40 cm/sec from one cassette to another (by an apparatus similar to a tape recorder). The direction of motion of the tape is automatically changed when it has been completely wound from the cassette. The total length of solid-state track detectors (glass, mica) placed along the tape is 80 cm in each of the two directions of motion. The half-life is determined from the distribution of the tracks in the detectors along the direction of motion of the tape. The great length of the tape successfully solves the problem of the suppression of the background from long-lived products.

The mechanical methods make it possible to detect the decay of nuclei with half-lives down to 0.1 nsec. In Ref. 68, this was achieved by constructing the target in the form of a disk of diameter 16 cm rotating at up to 24000 rpm.

The target is itself the collector of the recoil atoms. It is bombarded by a beam at an angle of 12° to the surface. This results in complete stopping of the recoil atoms, and the effective depth of the layer of the emission source for detection of the fission fragments by track detectors parallel to the surface of the target is only 1–2 mg/cm^2. As a result, the detection efficiency for spontaneous fission events is high.

Transport of Recoil Atoms in a Gas Medium. Various difficulties in the operation of mechanical collectors into which the recoil atoms strike directly arise from the high level of activation of the collector by the beam and from thermal heating. The range of the recoil atoms in the material of the collector may reach several mg/cm^2.[69] This large effective thickness of the radiation sources does not permit precision spectrometry of α-active and spontaneously fissioning products. These circumstances have led to the wide use in heavy-ion physics of transport of the products of nuclear reactions by means of gas media.

The first stage in all forms of these methods is the stopping of the recoil atoms knocked out of the target in the gas medium. The subsequent separation of the recoil atoms from the gas medium and concentration of them on a relatively small surface, which is necessary for efficient detection of the decay, can be done in several ways: a) by adsorption on the walls of the volume containing the gas[70]; b) by electrostatic collection on an electrode collector, since the thermalized recoil atoms carry electric charges in an appreciable fraction of the cases[71,72]; c) by adsorption from a gas jet (usually helium) produced by evacuation through a small opening or capillary.[75] It is this last method, which is known as the *helium jet method*, that is the most efficient and convenient for the synthesis of new isotopes and elements.[72,76,77]

An arrangement used for synthesizing and studying the α decay of transuranic elements at the Laboratory of Nuclear Reactions at Dubna is shown in Fig. 11.[78] In this case, a gas jet with velocity close to the velocity of sound is formed at an opening of diameter 0.5 mm and

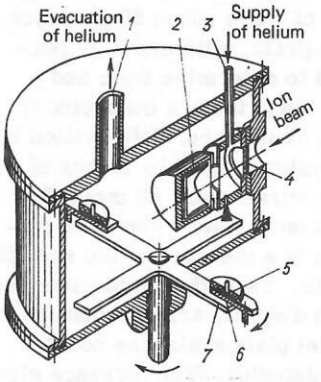

FIG. 11. Facility for studying α decay of transuranic elements. 1) Tube for evacuating helium from an opening of diameter 0.5 mm in the chamber with the target; 2) Faraday cylinder; 3) helium supply tube; 4) cassette with target; 5) silicon detector; 6) movable screen introduced by remote control between the collector and the detector during the detection of the α decay of the daughter nuclei; 7) collector of recoil atoms, which is periodically rotated through 90°.

depth 1 mm. On one side of this opening is a volume with gas pressure ~1 atm, in which the recoil atoms have been stopped. On the other side, a pressure ~1 torr is maintained by intense evacuation. The recoil atoms are adsorbed when the jet collides with an aluminum collector. A total collection efficiency of about 50% was maintained during many hours of operation with collection time <1 sec.

Later, to transport the recoil atoms, capillaries with diameter of the inner opening ~1 mm and length up to 200 m were used.[76] At the end of the capillary where the evacuation takes place, a laminar flow with velocity near the velocity of sound in the given gas is established. However, even at the start of the capillary the flow velocity is an appreciable fraction (~0.3) of the velocity of sound. In rough estimates, one can therefore assume that the time required to traverse the capillary is a few msec/m. In real systems, it proved possible to study nuclei with half-lives down to 0.5 msec.[79]

In general, the efficiency of collection of recoil atoms in systems with capillaries is somewhat less than when openings are used, but it can still reach several tens of percent. The main source of loss of recoil atoms in the capillary is turbulence. The transition from laminar to turbulent flow is governed by the Reynolds number

$$R = 2va\rho/\eta,$$

where v is the velocity of the flow in cm/sec, a is the radius of the capillary in cm, ρ is the density of the gas in g/cm^3, and η is the gas viscosity in poise. When $R > 1000$, the flow becomes turbulent. Typical systems with a helium jet have $R \approx 1000$. It is therefore necessary to eliminate restrictions in the capillary, mechanical vibration, sharp bends, and dirt. Teflon and polyethylene are most frequently used as the material of the capillaries.

It is now widely recognized that a helium jet takes up not isolated recoil atoms, but fairly large aerosol-type

clusters, on which the recoil atoms are adsorbed. It was established experimentally in Ref. 80 that the mass of these clusters is ~10^8 amu. The presence of such clusters in the volume in which the recoil atoms are thermalized is a necessary condition for a stable high coefficient of collection of recoil atoms. For work with a heavy-ion beam, clusters can be formed from different admixtures in the helium such as vapor of oil, water, ethanol and so forth.[77] Special aerosol generators also give good results. For example, a generator of oil aerosols producing a concentration 10^6 cm^{-3} in the thermalization volume made it possible to obtain a collection efficiency of the recoil atoms of 80% with variations of not more than ±1.5% over several days.[81]

When recoil atoms are adsorbed from a jet out of an opening or a capillary, the angle at which the jet approaches the surface of the collector is important. If there is a deviation of the jet from normal incidence, the efficiency falls off in proportion to the square of the sine of the angle.[82]

Separation of Complete Fusion Products in Electric and Magnetic Fields. This method has been developed in a number of laboratories to achieve reliable separation from the beam and subsequent identification of extremely short-lived products of complete fusion reactions. In the first place, they have been developed in connection with the synthesis of superheavy elements ($Z = 114-126$) in order to make possible identication of the elements for a lifetime down to about 10^{-7} sec.[83]

In 1976 SHIP, a separator of products of reactions induced by heavy ions, was put into operation on the heavy-ion accelerator at Darmstadt.[9,84,85] The schematic arrangement of SHIP is shown in Fig. 12.

The main parameters are as follows:

Size of target	0.3×1 cm^2
Axial and radial entrance apertures	3°
Exit slit	3×3 cm^2
Axial exit aperture	3.4°
Radial exit aperture	2.8°
Target–exit distance	11 m
Charge acceptance	20%
Velocity acceptance	10%

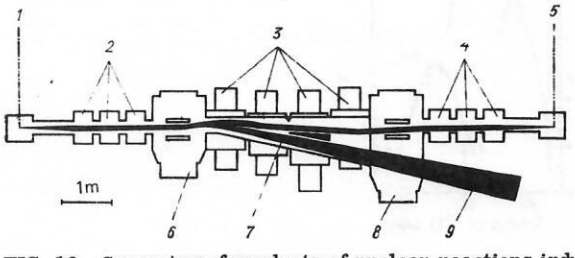

FIG. 12. Separator of products of nuclear reactions induced by heavy ions. 1) Target; 2) and 4) quadrupole triplets; 3) dipole magnets; 6) and 8) regions of the electric field; 7) slit for separating products with different velocities; 9) deflected ion beam.

Electric field:

distance between plates	15 cm
size of plates	50×60 cm^2
maximal voltage	800 kV

Dipole magnets:

area of pole (three magnets)	40×50 cm^2
area of hole (one magnet)	40×65 cm^2
gap width	15 cm
maximal field strength	0.7 T

Quadrupole magnets:

radius of aperture	7.5 cm
length of iron	25 cm
maximal gradient	9.5 T/m

The complete installation is a Wien velocity filter consisting of crossed homogeneous electric and magnetic fields.

The principle of operation of the Wien filter is as follows: ions with charge Z_i and velocity v that enter the filter at right angles to the electric and magnetic fields can pass undeflected through the filter only if $Z_i vB = Z_i E$, where B is the magnetic induction and E is the electric field intensity. We conclude from this that the filter selects particles with velocity $v = E/B$. The charge state of the particles plays no part.

In ordinary Wien filters, the regions occupied by the electric and magnetic fields coincide spatially. However, the products of reactions with heavy ions have high electric and magnetic rigidities: $BR \approx 1$ T·m and $ER \approx 10-20$ MV, where R is the radius of the particle trajectory when only one of the fields is switched on. To obtain the necessary electric field intensity (~500 kV across a gap of ~10 cm), one needs a large vacuum volume for the electrodes, and in the ordinary variant of the Wien filter it is necessary to obtain a field ~0.5 T in a gap ~50 cm. In SHIP, this problem was solved by separating spatially the regions occupied by the electric and the magnetic fields.

Testing of SHIP for the detection of the products of the $^{144}Sm(^{40}Ar, 7n)^{177}Hg$ reaction at argon energy 240 MeV showed that the beam separation is 10^{11}, and the efficiency of collection of recoil atoms is 5%.[84] Estimates show that for reactions with evaporation of one or two neutrons the efficiency of collection of the recoil atoms may be tens of percent.

When SHIP is used in experiments on the synthesis of superheavy elements, the identification is made by a measurement of the mass from the time of flight and also by determination of the charge of the nuclei by means of $\Delta E-E$ gas telescopes.

A Wien velocity filter with constant magnetic field and rf electric field has been put into operation at the Tandem Laboratory at the University of Munich.[86-88] The rated parameters of this installation as regards efficiency of recoil atom collection and degree of separa-

tion from the original beam are close to the values obtained with SHIP. The use of the rf field for separation from the original beam makes it possible to exploit not only the difference between the velocities of the initial particles and the reaction products, but also the difference between the times of arrival of the particles from the target and from the edges of the entrance collimators of the beam. The scattering on the entrance collimators of the separator makes the main contribution to the number of beam particles that pass through a filter with constant electric field. On the tandem at Munich, the necessary pulsing of the beam is ensured by an rf voltage of 10 MHz with amplitude 160 kV in the filter itself. The direct beam cannot pass through the filter when there is no voltage on it because of the geometry of the filter. Maximal separation of the rf-deflected particles is ensured by entry into the field region in antiphase at maximal field values. These conditions are most readily satisfied if the target and projectile have nearly equal masses, when the ratio of the velocities of the initial ions and the recoil atoms is close to two.

The rf filter at Munich was tested on the $^{12}C(^{12}C,x)$ reaction at energy 38.6 MeV. From 10^{15} particles that bombarded a target of thickness 145 $\mu g/cm^2$, 10^3 particles with energy near the initial energy reached the detector; there were 10^6 particles with energy around 8 MeV, and 5×10^5 particles that were complete fusion products.

Detection of the Decay of Nuclei with Lifetimes in the Range 10^{-7}–10^{-12} sec. In this time range, an appreciable number of fission isomers has been found.[89] We shall therefore consider variants of methods suitable for detecting their decay.

A method for detecting the fission fragments of a fission isomer with half-life 4.5×10^{-8} sec (Fig. 13a) is described in Ref. 90. The collimated beam of recoil atoms passes through a diaphragm and enters the vacuum chamber, which is surrounded on four sides by glass detectors having the form of a truncated pyramid with axis at the center of the target. The opening angle of the pyramid is chosen so that the products of the nuclear reactions do not strike the glass. The glass detectors detect the fission fragments of recoil atoms that decay in flight. The lower limit of the lifetime in this method was ~10^{-9} sec and the upper limit ~10^{-7} sec.

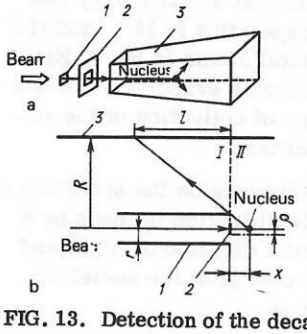

FIG. 13. Detection of the decay of fission isomers in flight. a) For the range of lifetimes 10^{-7}–10^{-9} sec: 1) target; 2) collimator; 3) glass detectors. b) For times down to 10^{-12} sec: 1) tube for fixing the target; 2) target; 3) solid-state detectors of the fission fragments; *I* is the region of detection of the fragments from delayed fission; *II* is the region of detection of fragments of induced fission.

A further development of this method was the so-called *projection method*,[91] the principle of which is shown in Fig. 13b. A target with radius $\rho\lesssim1$ mm is bombarded by a beam of ions. The tube in which the target is fixed has radius r. The detectors of the fission fragments are mounted on a cylinder at distance R from the beam axis. In this case, a recoil atom at distance x from the target emits fragments when it decays that will be detected at detector length $l=(R-r)x/r$. For $R=100$ mm and $r=1.15$ mm, 10 μm along the x axis corresponds to $l=0.86$ mm. Estimates show that the projection method can be used to measure lifetimes of fission isomers down to 5×10^{-12} sec. This was confirmed in Ref. 92, in which a fission isomer of ^{240}Cm was obtained with a half-life 10^{-11} sec.

Identification of Complete Fusion Products. The problem of identification is particularly important for the synthesis of new transuranic elements, but the basic methods of identification are the same for isotopes, transuranic elements, and lighter elements. In the present review, we shall consider only methods of identification of relatively short-lived isotopes ($T_{1/2}\lesssim1$ min), for which the ordinary chemical, mass-spectroscopic, and other methods are not sufficiently fast.

Measurement of excitation functions. The main method for obtaining isotopes of new transuranic elements is the complete fusion reaction, in which the compound nucleus sheds its excitation by emitting neutrons and γ rays. The dependence of the yield of such reactions on the projectile energy has a characteristic form of peaks with width ~10 MeV (FWHM), the position of the peaks in the energy scale being related to the number of evaporated neutrons. The excitation functions of the $^{238}U(^{18}O,xn)$ reaction are shown as an example in Fig. 14.[93]

As a rule, reactions with the emission of charged

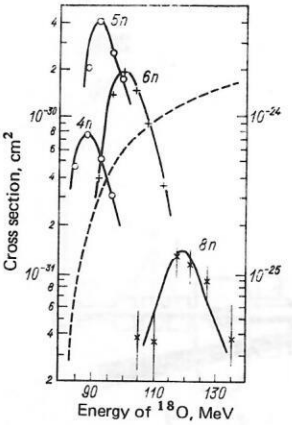

FIG. 14. Excitation functions of the $^{238}U(^{18}O,xn)$ reaction. The dashed curve shows the dependence of the cross section for production of the compound nucleus, the scale for which is given on the right.

particles or nucleon transfer reactions do not have such well-defined peaks in the excitation functions, although the dependence of their cross sections on the projectile energy may also be nonmonotonic.[94,95] The position and profile of the peaks of the excitation functions can be related to the number of evaporated neutrons by Jackson's computational method, which was first developed for reactions with protons and then modified to analyze reactions on heavy ions.[96,97]

The empirical Alexander–Simonoff relation,[98] which was carefully analyzed in Ref. 99, is also useful. In Ref. 99, there is an empirical formula for the mean energy carried away from the compound nucleus in the form of the kinetic energy of the neutron and the energy of γ rays in each step in the neutron evaporation cascade. The formula is $E=(8.98-0.024A^*)$ MeV, where A^* is the mass number of the compound nucleus. Using this formula, one can determine the position of the peaks in the excitation functions with the evaporation of different numbers of neutrons for a given target + ion combination and thereby, by comparison with the experimental results, determine the mass number of the obtained isotopes.

Reasonable agreement with the experimental data is also obtained in the statistical model of formation and decay of compound nuclei with the evaporation of particles calculated by the Monte Carlo method.[100]

Collimation method. The existence of almost 2000 radioactive isotopes has the consequence that the radioactive properties of new isotopes obtained in complete fusion reactions may be similar to the decay properties of lighter nuclei which can be produced in the same experiments in incomplete fusion reactions. To distinguish the products of complete and incomplete fusion, the difference between their angular distributions can be used.

Because the cross sections for the production of transuranic elements are small, it is difficult to measure the differential angular distributions of these elements. Therefore, for additional identification of the isotopes of the 102-th and 104-th elements in Ref. 101 a collimator in the form of a system of circular openings through plates of different thicknesses was placed behind the target on the side of the recoil atom collector. Depending on the ratio of the plate thickness to the diameter of the openings, products with different angular distributions will pass more or less readily through the collimator (Fig. 15).[101] On the one hand, the collimation method makes it possible to suppress the background from nucleon transfer reactions and, on the other, it gives an additional proof that the product was produced in a complete fusion reaction rather than in some other reaction.

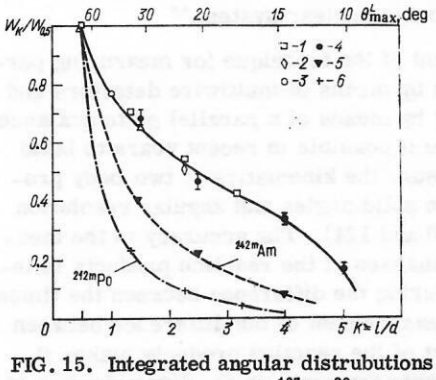

FIG. 15. Integrated angular distrubutions of products of complete fusion reactions. 1) ^{197}Au(^{22}Ne, $6n$, $5n$)^{213,214}Ac; 2) ^{238}U(^{16}O, $6n$)^{248}Fm; 3) ^{238}U(^{22}Ne, $4n$)^{256}102; 4) ^{239}Pu(^{18}O, $5n$)^{252}102 and many-nucleon transfers; 5) ^{242}Pu(^{22}Ne + p − n)^{242m}Am; 6) ^{208}Pb(^{22}Ne + 2p + 2n)^{212m}Po.

Crossed reactions. An important feature of reactions on heavy ions is the possibility that through combination of the target and the particle one and the same product can be obtained in different ways. This crossed production of the same product greatly increases the reliability of identification. For example, in Ref. 102 the isotope ^{254}102 was obtained in two reactions: ^{243}Am(^{15}N, $4n$) and ^{238}U(^{22}Ne, $6n$), for each of which the excitation function was measured. In Ref. 102, the method of crossed reactions in conjunction with the data of Ref. 78 made it possible to establish reliably the properties of the isotopes ^{254}102.

A carefully thought-out system of crossed reactions was used in Ref. 103 to synthesize isotopes of elements 103, 105, and 107. The targets were ^{203}Tl, ^{205}Tl, ^{206}Pb, ^{207}Pb, ^{208}Pb, ^{209}Bi and the projectiles were ^{50}Ti, ^{51}V, ^{54}Cr, ^{55}Mn.

Detection of daughter products. When an isotope of a new transuranic element with atomic number Z is synthesized, the nuclei of the element with atomic number $Z-2$ obtained as a result of its α decay usually has known radioactive properties. The experiment can be arranged in such a way that they can reach the collector of secondary nuclei only if they are produced by the decay of the parent nuclei. The detection of daugher nuclei with atomic number Z and mass number A establishes the synthesis of nuclei with atomic number $Z+2$ and mass number $A+4$. As collector of the daughter nuclei, one can use the surface of a silicon detector employed to detect the α decay of the initial products.[78] The daughter nuclei strike into the surface of the detector as a result of their recoil on the α decay of the initial nuclei when the α particle is emitted in the direction opposite to the detector. Removing the collector of the initial nuclei, one can detect the α decay of the daughter nuclei by means of the same detector. Identification through daughter nuclei can be realized not only for α decay but also for β decay and the emission of delayed protons.[104]

To determine the mass number of the daughter products ejected from the collector as a result of recoil, one can use the time-of-flight technique.[105] In these experiments, it is very important to obtain thin layers of the initial products, which can be realized in the helium jet method.

Detection of x rays. The development of semiconductor x-ray detectors has made it possible to use the characteristic x-ray spectra to identify transuranic elements in a number of cases.

The atomic numbers of isotopes of elements 102 and

104 were determined in Refs. 106 and 107 by detecting characteristic K-series x rays of the daughter nuclei in coincidence with α particles of the initial nuclei. This is possible if the α decay takes place to excited states of daughter nuclei that are de-excited in the internal conversion process. The K x rays are due to rearrangement of the atomic shells following the internal conversion on the K shell. Alpha decay to excited levels is characteristic of odd nuclei; measurements have been made with the isotopes $^{255}102$ ($T_{1/2} \approx 3$ min) and $^{257}104$ ($T_{1/2} \approx 4.5$ sec). The yield of K x rays per α decay for $^{255}102$ was 0.56 ± 0.04 and for $^{257}104$ it was 0.16 ± 0.04.

A mass separator working in the on-line regime for heavy-ion beams is a powerful tool for investigating the products and mechanisms of reactions induced by heavy ions.

The mass separators used for heavy-ion beams differ from the ones used for high-energy proton accelerators and reactors only by the details of the construction of the target and the ion source.[83,108] The high potential of mass separators for studying nuclei far from the β-stability line is demonstrated, for example, by the measurement[83] of the half-life of ^{11}Li (9.0 ± 0.5 msec) and the direct mass-spectroscopic measurement of its mass with an error not exceeding 100 keV.

The ion sources that have now been developed are characterized by a high selectivity with respect to the chemicophysical properties of the elements. With the mass separator EMSNAPTI[109] at the Laboratory of Nuclear Reactions at Dubna and different variants of gas-discharge ion sources it is possible to obtain a high yield (up to tens of percent) and counting rate (down to about 5 msec) for gases and volatile elements: radium, francium, astatine, polonium, lead, and thallium.[110,111] With the mass separator BÉMS-2 (see Refs. 112 and 113), which is also in operation at the Laboratory of Nuclear Reactions, a surface-ionization source ensures a separation efficiency up to tens of percent and a counting rate down to a few seconds for cesium, barium, and rare earth elements.

A promising direction for making ion sources that can be used for a large number of chemical elements and have a counting rate down to about 0.01 sec is based on direct transport of reaction products by means of a helium jet into the region of the ion source.[114] The investigation of Ref. 115 demonstrates the possibility of varied applications of mass separators in heavy-ion physics. From the isotope distributions of the additional fission fragments it was possible to determine with good accuracy the mean number of neutrons resulting from fission of the compound nucleus. The relations used have the form

$$^{182}_{74}\mathrm{W} + ^{40}_{18}\mathrm{Ar} \to ^{222}_{92}\mathrm{U}^* \to {}_{37}\mathrm{Rb} + {}_{55}\mathrm{Cs} + \nu;$$

$$^{158}_{64}\mathrm{Gd} + ^{22}_{10}\mathrm{Ne} \to ^{180}_{74}\mathrm{W}^* \to {}_{37}\mathrm{Rb} + {}_{37}\mathrm{Rb} + \nu.$$

Fast chemistry. The epithet "fast" is here used in the sense that the chemical operations can be made in a time of the order of seconds or minutes.

The most striking example of such chemistry is the chemical identification of elements 104 and 105 in isotopes with half-lives ~1 sec.[116,117] These experiments used the appreciable difference in the volatility of chlorides of actinides and transactinide elements. The recoil atoms knocked out of the target were thermalized in a nitrogen flow, and then mixed with a chlorinating agent. The gas flow together with the chlorides of the transuranic elements was fed into a thermochromatographic column, which was simply a glass tube up to 4 m long with a temperature gradient over its length from 300–400 °C to room temperature. Depending on their volatility, the compounds precipitated on sections with different temperatures. The correspondence of these sections to a particular element was calibrated by means of the chlorides of known elements—hafnium and tantalum, which are chemical analogs of elements 104 and 105. The spontaneous fission of nuclei precipitated on the walls of the column was detected by mica detectors placed directly in the column.

Significant progress has also been achieved in the chemistry of solutions. In Ref. 118, in the chemical identification of the isotope $^{261}104$ with half-life 65 sec, all chemical operations in the ion-exchange column, including drying of the samples for measurement of the α-particle spectra, were performed automatically in 2–3 min. The original collection of the recoil atoms was made by means of a helium jet. A review of the collection of recoil atoms in gas media for fast chemical operations is given in Ref. 77.

Investigation of the kinematics of the decay products of the compound nucleus. For heavy compound nuclei with $A \gtrsim 200$, the main process of their de-excitation is fission into two fragments of comparable mass. For understanding the interaction mechanism, it is important to establish the fact that what has fissioned is a nucleus produced by fusion of a target nucleus with the whole of the bombarding particle, and not merely part of it, and also that only two fragments are formed in the exit channel. In a two-body process, momentum conservation makes it possible, from measurement of the angular correlations of the fission fragments, to determine the contribution of incomplete fusion reactions.[119,120] The kinematic conservation laws in two-body processes are applied today not only to the fission of compound nuclei but also to deep inelastic nucleon transfer reactions which pass through the stage of formation of a double nuclear system.[12]

The development of the technique for measuring particle coordinates by means of multiwire detectors and the time of flight by means of a parallel plate avalanche counter has made it possible in recent years to build facilities to measure the kinematics of two-body processes with large solid angles and angular resolution 0.1° (see Refs. 10 and 121). The accuracy in the measurement of the masses of the reaction products is increased by measuring the difference between the times of flight.[10,122] Measurement of the difference between the times of flight of the reaction products makes it possible to eliminate the error in the determination of the masses by the ordinary time-of-flight technique resulting from inaccurate calibration of the detectors which measure the particle energies.

The difference method is based on comparison of the difference between the very accurately measured times of flight of the reaction products and their emission angles with calculated values obtained from the kinematic conservation laws under different assumptions about the masses of the reaction products.

4. MEASUREMENT OF THE LIFETIME BY THE DOPPLER-SHIFT METHOD AND BLOCKING TECHNIQUE

The Doppler shift is exploited to measure the lifetime in radiative transitions as follows.[123] Excited nuclei produced in a reaction receive a recoil momentum, are ejected from a thin target, and move in vacuum, emitting γ rays whose energy is shifted by the Doppler effect. To second order, the shift is determined by the expression

$$E = E_0(1+\beta\cos\theta-\beta^2/2+\beta^2\cos^2\theta),$$

where $\beta = v/c$ is the ratio of the velocity of the recoil atom to the velocity of light, and θ is the angle between the direction of v and the wave vector.

Placing a stopper of the recoil atoms at different distances behind the target, one can stop some of the recoil atoms before they emit γ rays. A Ge(Li) detector placed at angle 0° to the beam measures the relative intensities of the γ rays from the moving and stopped nuclei. Changing the distance between the target and the stopper, one can obtain the decay curve of the excited state.

For the lifetime range 10^{-9}–10^{-12} sec and velocity of the recoil atoms of the order of a few percent of the velocity of light, the distance between the target and the stopper lies between several microns and several millimeters. The γ-ray spectra for transitions between rotational levels in ^{160}Er for different distances between the target and stopper are shown in Fig. 16, which is taken from Ref. 124. The ^{124}Sn(^{40}Ar, $4n$)^{160}Er reaction was studied. The lifetimes for the $2^+ \to 0^+$, $4^+ \to 2^+$, $6^+ \to 4^+$, and $8^+ \to 6^+$ transitions are, respectively, $(910 \pm 140) \times 10^{-12}$ sec, $(37 \pm 6) \times 10^{-12}$ sec, $(5.9 \pm 1.2) \times 10^{-12}$ sec, and $(2.4 \pm 0.5) \times 10^{-12}$ sec.

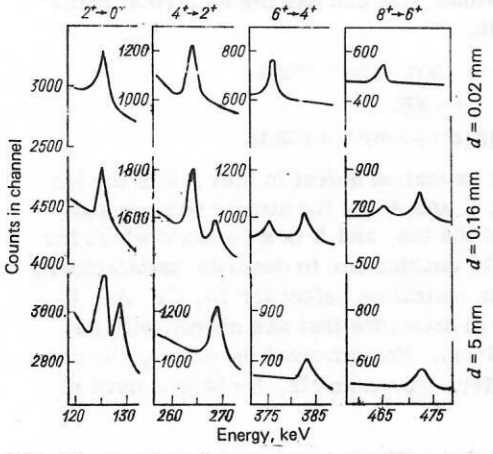

FIG. 16. Spectra of γ rays for transitions between rotational levels in ^{160}Er for different distances d between the target and stopper.

The idea of the blocking technique is as follows.[125,126] The nuclear reaction is studied in a single crystal. The compound nucleus is displaced from the lattice sites because of the projectile momentum. At the time of decay, the compound nucleus has moved on the average from the site through a distance $S = V\tau$, where V is its velocity and τ is its mean lifetime.

Charged particles emitted by nuclei at the sites of the crystallographic lattice in the directions of the crystallographic axes and planes are strongly scattered already on the nearest nuclei. The angular distributions of the particles that leave the crystal therefore exihibit regions with much reduced intensity of the particles; these "shadows" are arranged in a manner determined by the structure of the crystal. The displacement of the nuclei from the site changes the shape of the shadows in the angular distributions of the decay products, and, for known velocity of the recoil nucleus, one can determine τ from these changes. The range of times that can be measured by this effect in reactions induced by heavy ions is 10^{-16}–10^{-19} sec.

The angular distributions of the fragments of W fission by ^{31}P ions with energy 195 MeV near the ⟨111⟩ crystallographic axes of a W single crystal oriented at the angles 90° and 160° to the ion beam are shown in Fig. 17.[127] The measurements were made by means of glass detectors of the fission fragments. The difference between the relative depths $\Delta\chi$ of the shadows (the intensities of the particles at the minima of the angular distributions) for different orientations of the crystal is a function of $v\tau$. For small displacements of the nuclei from the lattice sites of ~0.1 of the interatomic spacing, this dependence has the form

$$\Delta\chi = 2CN\pi d\,(\sin^2 90° - \sin^2 160°)\,(v\tau)^2,$$

where C is a semiempirical parameter equal to 2.5, N is the number of atoms in 1 cm^3 of the single crystal, and d is the interatomic distance for the chosen crystallographic axis. Using Fig. 16, we find $\tau \approx 10^{-18}$ sec. However, the connection between the profile of the shadow and the lifetime of the compound nucleus has not been sufficiently investigated, and this leads to large uncertainties in the values of τ.

5. SILICON DETECTORS IN HEAVY-ION PHYSICS

Among the numerous parameters involved in the wide use of silicon detectors for the detection of heavy ions,

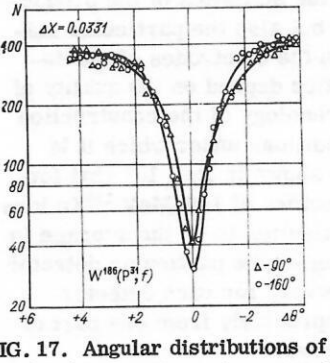

FIG. 17. Angular distributions of the fission fragments near the ⟨111⟩ crystallographic axis of a W single crystal orientated at different angles to a beam of 195-MeV ^{31}P ions.

the most specific are the following: a) the limiting energy resolution; c) the radiation stability.

Limiting Energy Resolution. Modern electronics makes it possible to reduce the contribution of noise to the detector resolution to not more than 0.1 keV. Therefore, the contribution of electronic noise in the detection of heavy ions with energies between tens and hundreds of MeV can be ignored. The contribution from the fluctuations in the production of charge carriers with the Fano factor adopted for silicon, $F \approx 0.075$, is determined by the expression[35]

$$\delta\,(\mathrm{FWHM,keV}) = [1.5E(\mathrm{MeV})]^{1/2}.$$

For $E = 100$ MeV, for example, we obtain accordingly $\delta = 12$ keV, i.e., about 0.012%.

The main factor determining the limiting resolution in the detection of heavy ions is nuclear collisions. Fluctuations of the energy loss accompanying nuclear collisions leads to an energy spread that for $A \lesssim 10$ is determined by the expression[129]

$$\delta_n\,(\mathrm{FWHM,keV}) = 0.7Z^{1.2}A^{4/3}.$$

Hence, already for boron ions B we obtain $\delta_n = 34$ keV. For heavier ions, we use estimates of the effect of nuclear collisions given in Ref. 130, from which it follows that $\delta_n = 90$ keV for ^{24}Mg, $\delta_n = 0.5$ MeV for ^{80}Br, and $\delta_n = 5$ MeV for ^{238}U. Since the effect of nuclear collisions is most important at the end of the range, the above estimates for δ_n can be assumed to be independent of the energy of the ions in the energy range 1 MeV/nucleon $\lesssim E \lesssim$ 10 MeV/nucleon.

For silicon ΔE detectors, if channeling is eliminated, the main factor that determines the limiting energy resolution is associated with fluctuations in the energy loss of a particle in the detector as an absorber. Accordingly, to estimate the limiting resolution, one can use the relation[8]

$$\delta\,(\mathrm{FWHM,keV}) = 0.924Z_1\,(Z_2\Delta x/A_2)^{1/2},$$

where Z_2A_2 refers to the material of the absorber of thickness Δx μg/cm^2, and Z_1 is the atomic number of the particle. For the particular case of silicon,

$$\delta\,(\mathrm{FWHM,keV}) \approx 10Z_1\,[\Delta x\,(\mu\mathrm{m})]^{1/2}.$$

It should, however, be noted that the resolution obtained in practice in the detectors does not correspond to the best possible value. This comes about because one must contend with not only the statistics of the production of the charge carriers but also the particular statistics of their collection on the electrodes of the detector. These latter statistics depend on the quality of the original silicon, the technology of the construction of the detector, and the conditions under which it is used. For example, it was shown in Ref. 131 that for the detection by silicon detectors of 149-MeV ^{136}Xe ions the efficiency of carrier collection is on the average in the range 60–95%, depending on the particular detector and the applied bias. Moreover, for each detector these numbers may vary appreciably from one part of the sensitive volume to another.

Ionization Defect. This effect introduces important limitations in the accuracy with which the energy of the heaviest ions can be determined by means of silicon detectors. The ionization defect is usually defined as the difference between the energies of α particles and heavy ions that give pulses of the same amplitude in the detector. In other words, it is the underestimation of the energy of a heavy ion measured by a detector calibrated by means of α particles. According to the data of Ref. 132, the ionization defect for sulfur and aluminum ions is ~0.5 MeV, for nickel ions it is ~2 MeV, for silver ions ~4 MeV, and for uranium ions ~10 MeV. According to the data of various investigators, these numbers fluctuate somewhat, but the order of magnitude remains the same. In the total ionization defect, one usually distinguishes the contribution from the energy loss in the entrance window, the contribution from the energy loss in nuclear collisions, and a residual defect, which is largely due to recombination of carriers in the plasma produced by the heavy charged particle. These contributions to the total ionization defect are comparable in magnitude. It should be noted that the width of the effective entrance layer of the detector for heavy ions is 5–10 times greater than for α particles. Recombination effects are particularly important precisely near the surface of the detector.[131,133] In accordance with Ref. 134, the recombination contribution to the ionization defect is

$$\Delta \sim \mathscr{E}S^2/(t_0E^2),$$

where $\mathscr{E}$ is the energy of the particle, S is the specific energy loss of the particle, t_0 is the lifetime of the minority carriers in silicon, and E is the field intensity in the detector. Therefore, to reduce the ionization defect one should operate at high electric field intensities in the detector and use silicon with a large value of t_0 in the detectors.

The value of the ionization defect for each particular detector and its dependence on Z and A for the detected particles is best determined experimentally. The corresponding procedure is described, for example, in Ref. 135, in which the ions ^{22}Ne, ^{40}Ar, ^{84}Kr, ^{132,136}Xe, and ^{208}Pb with energies determined independently in different ways were used to calibrate the detectors. However, in view of the practical difficulties in the way of such calibrations, one can use the empirical relations of Ref. 136:

$$\mathrm{ID} = [6\varepsilon^{1.407}(\varepsilon+8) + B'(1+525\varepsilon^{-1.407})]/K;$$
$$\varepsilon = K\mathscr{E};$$
$$K = 6.53\cdot 10^4/[Z\,(Z^{2/3}+5.81)^{1/2}\,(A+28.1)].$$

Here, ID is the ionization defect in MeV, $\mathscr{E}$ is the ion energy in MeV, Z and A are the atomic number and mass number of the ion, and B is a constant which for a value $B = 13$–15 enables one to describe satisfactorily the values of the ionization defect for Ni, Cu, Ag, I, Au, and U ions in detectors that use silicon with resistivity ~500 $\Omega\cdot$cm. For different detectors, the constant B may differ. For example, $B = 18$ was used in Ref. 137.

Radiation Stability. The formation of defects in the crystal lattice under the influence of the heavy ions is a serious restriction on the duration of operation of

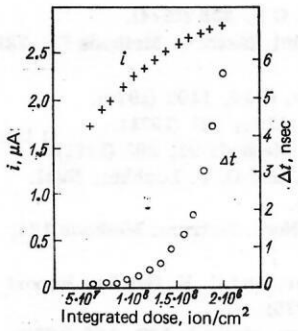

FIG. 18. Change in the properties of a silicon detector bombarded by 117-MeV iodine ions.

silicon detectors under high loads. The change in the properties of a surface barrier detector of the firm ORTEC due to bombardment with 117-MeV iodine ions is shown in Fig. 18.[53,138] The detector area was 50 mm^2, the silicon had resistivity 1 $k\Omega \cdot cm$, and the bias was 60 V. The leakage current (and accordingly, the energy resolution) and the shift of the time signal changed appreciably already at an integrated flux of 1×10^8 cm^{-2}.

In Ref. 139, in a test of ΔE detectors, it was found that at an integrated flux 10^9 cm^{-2} of 86-MeV ^{10}Be ions there is an increase of the reverse current in the detectors, a reduction in the signal amplitude, and a deterioration of the energy resolution. Thus, if there is not to be a serious deterioration in their properties, silicon detectors can operate only up to integrated fluxes of not more than 10^8–10^9 cm^{-2}.

6. PHOTOEMULSION METHOD AND DIELECTRIC DETECTORS

The majority of experiments in heavy-ion physics is made by electronic methods. However, in some cases valuable information can be obtained by photoemulsions and solid-state track detectors (glass, mica, plastic, and minerals). Many-particle processes recorded in a photographic emulsion and resulting from the interaction of 200-MeV ^{20}Ne ions with Ag and Br nuclei are shown in Fig. 19 (from Ref. 140).

The determination of Z of heavy ions with energy <10 MeV/nucleon in photographic emulsions is not simple because of the high ionization density produced by such particles in the emulsion and the strong velocity dependence of the effective charge. However, important progress has been made in this direction too.

The method of discrimination of the tracks of heavy

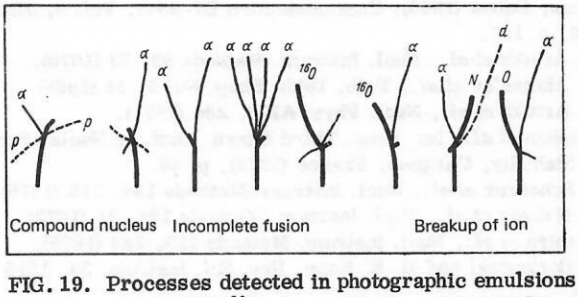

FIG. 19. Processes detected in photographic emulsions for interaction of 200-MeV ^{20}Ne ions with Br and Ag nuclei.

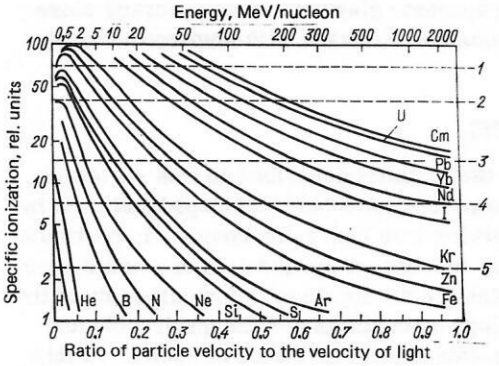

FIG. 20. Threshold detection levels for heavy ions by different solid-state detectors. A particle having initial specific ionization above the level indicated by the dashed line produces damage in the detector that appears as a track on etching; 1) meteoritic minerals; 2) glass, mica; 3) Dacron, mylar; 4) polycarbonate; 5) cellulose nitrate.

ions on the basis of the specific energy losses in a fine-grain low-sensitivity emulsion makes it possible to determine the atomic numbers of the heavy ions to within ±2 up to $Z \approx 30$.[141] A review of the numerous possibilities of the photoemulsion method not yet exhausted can be found in the fundamental book of Ref. 142.

Immediately after its development, the method of solid-state track detectors found wide application in heavy-ion physics.[143,144]

These detectors are characterized by a threshold sensitivity for heavy charged particles, relative simplicity of the evaluation and scanning, low intrinsic background, high detection efficiency, the possibility of using detectors of the most varied shape and size, and the ability to retain for a long period recorded information.

The wide choice of solid-state detectors with different sensitivity thresholds for detection of heavy ions with different charges and energies is illustrated in Fig. 20, which is taken from Ref. 143. Each detector has a threshold for the specific ionization, below which the tracks are not revealed by etching and above which all particles give tracks on etching. The range of particles that can be detected in solids extends from protons to ions of the transuranic elements. The threshold properties of such detectors made it possible in Ref. 145, for example, to measure the cross section for complete fusion of ^{12}C, ^{16}O, and ^{20}Ne ions with Cu, Ag, Au, and Bi nuclei by detecting the recoil atoms in mica placed directly below the ion beam.

Selective chemical etching of solid-state detectors makes it possible to identify the atomic numbers of the detected particles, since the revealed length of the track is proportional to the Z of the particle stopped in the volume of the detector.[146]

Spectrometric measurements can also be made by means of solid-state detectors. For example, it was shown in Refs. 147 and 148 that by measuring the diameters of the etched tracks of fission fragments in glass one can determine their energy to an accuracy of 1–2 MeV. The energy spectra of the framgnets of the spontaneous fission of ^{252}Cf measured in these investigations

by means of phosphate glasses had an accuracy close to that of measurements made with semiconductor detectors.

CONCLUSIONS

Of course, the methods described in this review do not exhaust those that have been developed and used by physicists working with heavy-ion beams. In particular, we have hardly touched on the question of γ and β spectroscopy, which yields important information about the excitation of high-spin states and the quadrupole and magnetic moments of excited states of nuclei. In this field, the experimental techniques are much closer to those used in reactions induced by lighter particles. The fundamental books of Refs. 149 and 150 have already considered these questions.

The questions discussed in this review are the ones that are specific to heavy-ion physics. I hope that their brief presentation in the present paper will help in the optimal formulation of future experiments.

I am very grateful to V. V. Volkov and Yu. Ts. Oganesyan for valuable comments when this draft was being prepared.

[1]G. N. Flerov, in: Materialy konferentsii po yadernym reaktsiyam s mnogozaryadnymi ionami, Dubna (1958) (Proc. Conf. on Nuclear Reactions with Multiply Charged Ions, Dubna, 1958); Soobshchenie (Communication) R-374, JINR, Dubna (1959), p. 8.
[2]J. H. Fremlin, in: Nuclear Reactions, Vol. 1 (eds. P. M. Endt and M. Demeur), North-Holland, Amsterdam (1959) (Russian translation published by Gosatomizdat, Moscow (1962), p. 89).
[3]G. N. Flerov, in: Trudy Pyatogo Vsesoyuznogo soveshchaniya po uskoritelyam zaryazhennykh chastits (Proc. Fifth All-Union Conf. on Charged-Particle Accelerators), Dubna (1976).
[4]A. Hrynkiewicz, R. Broda, and J. Wilczynski, Fiz. Elem. Chastits At. Yadra 8, 397 (1977) [Sov. J. Part. Nucl. 8, 164 (1977)].
[5]R. Bock *et al.*, GSI-Bericht P-5-77, Darmstadt (1977).
[6]A. M. Baldin, Fiz. Elem. Chastits At. Yadra 8, 429 (1977) [Sov. J. Part. Nucl. 8, 175 (1977)].
[7]K. H. Kaun, P. Manfrass, and W. Frank, Fiz. Elem. Chastits At. Yadra 8, 1246 (1977) [Sov. J. Part. Nucl. 8, 512 (1977)].
[8]F. S. Goulding and B. G. Harvey, Ann. Rev. Nucl. Sci. 25, 167 (1975).
[9]P. Armbruster, in: Proc. Third Intern. Conf. on Nuclei Far from Stability, Cargese, France (1976).
[10]P. Armbruster, in: Proc. European Conf. on Nuclear Physics with Heavy Ions, Caen, France (1976).
[11]V. V. Volkov, Fiz. Elem. Chastits At. Yadra 6, 1040 (1975) [Sov. J. Part. Nucl. 6, 420 (1975)].
[12]V. V. Volkov, Nucleonika, 21, 53 (1976).
[13]W. U. Schröder and J. R. Huizenga, Ann. Rev. Nucl. Sci. 27, 465 (1977).
[14]G. N. Simonoff and J. M. Alexander, Phys. Rev. B 133, 104 (1964).
[15]V. A. Druin, S. A. Karamyan, and Yu. Ts. Oganesyan, Preprint 1670 (in Russian), JINR, Dubna (1964).
[16]C. E. Anderson, D. A. Bromley, and M. Sachs, Nucl. Instrum. Methods 13, 238 (1961).
[17]M. W. Sachs, C. Chasman, and D. A. Bromley, Phys. Rev. B 139, 92 (1965); Nucl. Instrum. Methods 41, 213 (1966).
[18]J. Cerny *et al.*, Nucl. Instrum. Methods 45, 337 (1967).
[19]J. B. Bowman *et al.*, Phys. Rev. C 9, 836 (1974).
[20]D. Bird and R. W. Ollerhead, Nucl. Instrum. Methods 71, 231 (1968).
[21]M. C. Lemaire *et al.*, Phys. Rev. C 10, 1103 (1974).
[22]A. G. Artukh *et al.*, Nucl. Phys. A168, 321 (1971).
[23]H. Pleyer *et al.*, Nucl. Instrum. Methods 96, 263 (1971).
[24]V. V. Avdeichikov, E. A. Ganza, and O. V. Lozhkin, Nucl. Instrum. Methods 131, 61 (1975).
[25]M. M. Fowler and R. C. Jared, Nucl. Instrum. Methods 124, 341 (1975).
[26]J. Barrette, P. Braun-Munzinger, and C. K. Gelbke, Report MPI-H-1975-V2, Heidelberg (1975).
[27]K. Sistemich *et al.*, Nucl. Instrum. Methods 133, 163 (1976).
[28]A. G. Artukh *et al.*, Preprint E7-10464, JINR, Dubna (1977).
[29]W. Pfeffer *et al.*, GSI-Bericht JI-76, Darmstadt (1976), p. 20.
[30]A. A. Vorob'ev and V. A. Korolev, Prib. Tekh. Eskp. No. 4, 42 (1961).
[31]T. D. Thomas *et al.*, Phys. Lett. B27, 504 (1968).
[32]P. Glässel, R. C. Jared, and L. G. Moretto, Nucl. Instrum. Methods 142, 569 (1977); Preprint LBL-5064 (1976).
[33]C. Tschalär, Nucl. Instrum. Methods 61, 141 (1968).
[34]P. Armbruster *et al.*, Nucl. Instrum. Methods 132, 129 (1976).
[35]Yu. K. Akimov *et al.*, Poluprovodnikovye detektory yadernykh chastits i ikh primenenie (Semiconductor Detectors of Nuclear Particles and their Use), Atomizdat, Moscow (1967).
[36]M. Moszynski and B. Bengston, Nucl. Instrum. Methods 142, 417 (1977).
[37]M. L. Muga *et al.*, Nucl. Instrum. Methods 83, 135 (1970).
[38]C. K. Gelbke, K. D. Hildebrandt, and R. Bock, Nucl. Instrum. Methods 95, 397 (1971).
[39]T. M. Cormier *et al.*, Nucl. Instrum. Methods 119, 145 (1974).
[40]A. B. Whitehead, IEEE Trans. Nucl. Sci. 13, No. 1, 747 (1966).
[41]V. M. Agranovich *et al.*, Zh. Eksp. Teor. Fiz. 57, 401 (1969) [Sov. Phys. JETP 30, 220 (1970)].
[42]H.-G. Clerc *et al.*, Nucl. Instrum. Methods 113, 325 (1973); GSI-Bericht 73-13, Darmstadt (1973), p. 31.
[43]A. A. Vorob'ev *et al.*, At. Energ. 27, 31 (1969).
[44]W. Lang and H.-G. Clerc, Nucl. Instrum. Methods 126, 535 (1975).
[45]W. F. W. Schneider, B. Kohlmeyer, and R. Bock, Nucl. Instrum. Methods 87, 253 (1970).
[46]W. Pfeffer, B. Kohlmeyer, and W. F. W. Schneider, Nucl. Instrum. Methods 107, 121 (1973).
[47]D. J. Ruggeri, IEEE Trans. Nucl. Sci. 19, No. 3, 74 (1972).
[48]G. Gabor *et al.*, Nucl. Instrum. Methods 130, 65 (1975).
[49]A. M. Zebelman *et al.*, Nucl. Instrum. Methods 141, 439 (1977).
[50]H. Stelzer, Nucl. Instrum. Methods 133, 409 (1976).
[51]B. Martin *et al.*, GSI-Bericht J-1-77, Darmstadt (1977), p. 148.
[52]U. Lynen and H. Stelzer, GSI-Bericht J-1-77, Darmstadt (1977), p. 147.
[53]W. F. W. Schneider *et al.*, Nucl. Instrum. Methods 123, 93 (1975).
[54]J. C. Jackmart *et al.*, in: Proc. Intern. Conf. on Heavy Ion Physics, Dubna (1966); Communication D7-5342, Vol. 3, JINR (1970), p. 137.
[55]A. G. Artukh *et al.*, Nucl. Instrum. Methods 82, 73 (1970).
[56]N. G. Afanas'ev *et al.*, Prib. Tekh. Eksp. No. 5, 44 (1966).
[57]A. G. Artukh *et al.*, Nucl. Phys. A176, 284 (1971).
[58]C. Stephan *et al.*, in: Proc. Third Intern. Conf. on Nuclei Far from Stability, Cargese, France (1976), p. 46.
[59]H. J. Scheerer *et al.*, Nucl. Instrum. Methods 136, 213 (1976).
[60]B. G. Harvey *et al.*, Nucl. Instrum. Methods 104, 21 (1972).
[61]D. Shapira *et al.*, Nucl. Instrum. Methods 129, 123 (1975).
[62]C. J. Borkowski and M. K. Kopp, Rev. Sci. Instrum. 39, 1515 (1968).

[63]V. A. Biryukov, V. G. Zinov, and A. D. Konin, Zh. Eksp. Teor. Fiz. **58**, 104 (1970) [Sov. Phys. JETP **31**, 59 (1970)].
[64]M. Mutterer *et al.*, GSI-Bericht J1-76, Darmstadt (1976), p. 8.
[65]G. Charpak *et al.*, Nucl. Instrum. Methods **62**, 262 (1968).
[66]H. Sann *et al.*, Nucl. Instrum. Methods **124**, 509 (1975).
[67]V. A. Druin *et al.*, Yad. Fiz. **24**, 254 (1976) [Sov. J. Nucl. Phys. **24**, 131 (1976)]
[68]G. M. Ter-Akopyan *et al.*, Nucl. Phys. **A255**, 509 (1975).
[69]L. C. Northcliffe and R. F. Shilling, Nucl. Data, Sect. A **7**, 233 (1970).
[70]E. D. Donets, V. A. Shchegolev, and V. A. Ermakov, At. Energ. **16**, 195 (1964).
[71]A. Ghiorso *et al.*, Phys. Rev. Lett. **1**, 18 (1958).
[72]V. L. Mikheev, Prib. Tekh. Eksp. No. 4, 22 (1966).
[73]A. M. Friedman and W. C. Mohr, Nucl. Instrum. Methods **17**, 78 (1962).
[74]V. A. Druin, N. K. Skobelev, and G. Ya. Sun Tszin-Yan, At. Energ. **26**, 374 (1969).
[75]R. D. Macfarlane and R. D. Griffioen, Nucl. Instrum. Methods **24**, 461 (1963).
[76]R. D. Macfarlane and W. C. McHarris, in: Nuclear Spectroscopy and Reactions (ed. J. Cerny), Part A, Academic Press, New York and London (1974), p. 243.
[77]N. Trautmann, in: Proc. Third Intern. Conf. on Nuclei Far from Stability, Cargese (1976), p. 30.
[78]B. A. Zager *et al.*, At. Energ. **20**, 230 (1966).
[79]K. Valli and E. K. Hyde, Phys. Rev. **176**, 1377 (1968).
[80]H. Jungclas, R. D. Macfarlane, and Y. Fares, Phys. Rev. Lett. **27**, 556 (1971).
[81]H. Wollnik *et al.*, Nucl. Instrum. Methods **127**, 539 (1975).
[82]W. J. Wiesehahn, G. Bischoff, and J. M. D'Auria, Nucl. Instrum. Methods **124**, 221 (1975).
[83]R. Klapisch, in: Nuclear Spectroscopy and Reactions (ed. J. Cerny), Part A, Academic Press, New York and London (1947), p. 213.
[84]H. Ewald *et al.*, in: Comm. European Conf. on Nuclear Physics with Heavy Ions, Caen, France (1976), p. 183.
[85]H. Ewald *et al* , Kerntechnik **16**, 237 (1964).
[86]D. Evers *et al.*, Jahresbericht 1975, Beschleunigerlabor der Universität und Technischen Universität, München, p. 169.
[87]S. Scorka, K. Rudolph, and J. Hertel, GSI-Bericht 73-3, Darmstadt (1973), p. 1.
[88]E. Kankeleit, F. R. Krueger, and B. I. Persson, Nucl. Instrum. Methods **121**, 321 (1974).
[89]H. C. Britt, At. Data Nucl. Data Tables **12**, 407 (1973).
[90]Yu. P. Gangrskiĭ *et al.*, Izv. Akad. Nauk SSSR, Ser. Fiz. **32**, 1644 (1968).
[91]V. Metag *et al.*, Nucl. Instrum. Methods **114**, 445 (1974).
[92]G. Sletten, V. Metag, and E. Liukkonen, Phys. Lett. **B60**, 153 (1976).
[93]E. D. Donets, V. A. Shchegolev, and V. A. Ermakov, Yad. Fiz. **2**, 1015 (1965) [Sov. J. Nucl. Phys. **2**, 723 (1966)].
[94]T. Sikkeland, N. H. Shafrir, and N. Trautmann, Phys. Lett. **B42**, 201 (1972).
[95]A. G. Artyukh *et al.*, Yad. Fiz. **19**, 54 (1974) [Sov. J. Nucl. Phys. **19**, 28 (1974)].
[96]T. Sikkeland, A. Ghiorso, and M. J. Nurmia, Phys. Rev. **172**, 1232 (1968).
[97]A. S. Il'inov, Soobshchenie (Communication) R7-7108, JINR, Dubna (1973).
[98]J. M. Alexander and G. Simonoff, Phys. Rev. B **133**, 93 (1964).
[99]W. Neubert, Nucl. Data Tables **11**, 531 (1973).
[100]V. S. Barashenkov *et al.*, Soobshchenie (Communication) R-7-7165, JINR, Dubna (1973).
[101]Yu. Ts. Oganesyan *et al.*, At. Energ. **28**, 393 (1970).
[102]E. D. Donets, V. A. Shchegolev, and V. A. Ermakov, At. Energ. **20**, 223 (1966).
[103]Yu. Ts. Oganessian *et al.*, Nucl. Phys. **A273**, 505 (1976).
[104]D. D. Bogdanov *et al.*, Yad. Fiz. **6**, 1113 (1967) [Sov. J. Nucl. Phys. **6**, 807 (1968)].
[105]H. Wollnik, Nucl. Instrum. Methods **139**, 311 (1976).
[106]P. F. Dittner *et al.*, Phys. Rev. Lett. **26**, 1037 (1971).
[107]C. E. Bemis *et al.*, Phys. Rev. Lett. **31**, 647 (1973).
[108]H. L. Ravn, in: Proc. Third Intern. Conf. on Nuclei Far from Stability, Cargese, France (1976), p. 15.
[109]N. I. Tarantin *et al.*, Nucl. Instrum. Methods **38**, 103 (1965).
[110]N. S. Ivanov *et al.*, At. Energ. **41**, 352 (1976).
[111]A. P. Kabachenko *et al.*, At. Energ. **41**, 353 (1976).
[112]V. A. Karnaukhov *et al.*, Nucl. Instrum. Methods **120**, 69 (1974).
[113]D. D. Bogdanov *et al.*, Nucl. Instrum. Methods **136**, 433 (1976).
[114]W.-D. Schmidt-Ott *et al.*, Nucl. Instrum. Methods **124**, 83 (1975).
[115]P. Klapisch *et al.*, Soobshchenie (Communication) R7-9994, JINR, Dubna (1976).
[116]G. N. Flerov and I. Zvara, Soobshchenie (Communication) D7-6013, JINR, Dubna (1971).
[117]I. Zvara, in: Prognozirovanie v uchenii o periodichosti (Prediction in the Study of Periodicity), Nauks, Moscow (1976), p. 92.
[118]E. K. Hulet *et al.*, in: Proc. Fourth Intern. Transplutonium Element Symposium, Baden-Baden (1975).
[119]T. Sikkeland and V. E. Viola, in: Proc. Third Conf. on Reactions between Complex Nuclei, Asilomar, 1963, Univ. of California Press (1963), p. 232.
[120]S. A. Karamyan *et al.*, Yad. Fiz. **9**, 715 (1969) [Sov. J. Nucl. Phys. **9**, 414 (1969)].
[121]R. Bock *et al.*, Report on the Ninth Masurian School in Nuclear Physics, Mikolaiki, Poland (1976).
[122]C. Cabot *et al.*, Nucl. Instrum. Methods **114**, 41 (1974).
[123]D. B. Rossan and E. K. Warburton, in: Nuclear Spectroscopy and Reactions (ed. J. Cerny), Part C, Academic Press, New York and London (1974), p. 307.
[124]B. Bochev *et al.*, Soobshchenie (Communication) R6-6229, JINR, Dubna (1972).
[125]S. A. Karamyan, Yu. V. Mekokov, and A. F. Tulinov, Fiz. Elem. Chastits At. Yadra **4**, 456 (1973) [Sov. J. Part. Nucl. **4**, 196 (1973)].
[126]W. M. Gibson, Ann. Rev. Nucl. Sci. **25**, 465 (1975).
[127]V. V. Kamanin *et al.*, Yad. Fiz. **16**, 447 (1972) [Sov. J. Nucl. Phys. **16**, 249 (1973)].
[128]Yu. V. Melikov *et al.*, Nucl. Phys. **A180**, 241 (1972).
[129]J. Lindhard and V. Nielsen, Phys. Lett. **2**, 209 (1962).
[130]E. L. Haines and A. B. Whitehead, Rev. Sci. Instrum. **37**, 190 (1966).
[131]V. F. Kushniruk and Yu. P. Kharitonov, Prib. Tekh. Eksp. No. 4, 76 (1977).
[132]B. D. Wilkins *et al.*, Nucl. Instrum. Methods **92**, 381 (1971).
[133]S. A. Kassirov *et al.*, Nucl. Instrum. Methods **119**, 301 (1974).
[134]E. C. Finch, Nucl. Instrum. Methods **113**, 41 (1973).
[135]Kh. Zodan *et al.*, Soobshchenie (Communication) R7-10671, JINR, Dubna (1977).
[136]S. B. Kaufman *et al.*, Nucl. Instrum. Methods **115**, 47 (1974).
[137]R. P. Schmitt *et al.*, Nucl. Phys. **A279**, 141 (1977).
[138]W. Pfeffer *et al.*, GSI-Bericht 73-14, Darmstadt (1973), p. 16.
[139]M. É. Kaganskaya, A. V. Kolodin, and M. A. Sychkov, Prib. Tekh. Eksp. No. 6, 55 (1973).
[140]R. Pfohl, Thesis, Strasbourg (1964).
[141]V. P. Perelygin, S. P. Tret'yakova, and M. D. Nikitin, Avt. svidetel'stvo SSSR 233113 (Inventor's Certificate SSSR 233113), Byull. OIPTZ No. 2, 63 (1969).
[142]C. F. Powell, P. H. Fowler, and D. H. Perkins, The Study of Elementary Particles by the Photographic Method, London (1959) (Russian translation published by Izd. Inostr. Literatury (1962)).
[143]R. L. Fleischer, P. B. Price, and R. M. Walker, Nuclear Tracks in Solids, University of California Press, Berkeley-Los Angeles-London (1975).
[144]V. A. Nikolaev and V. P. Perelygin, Prib. Tekh. Eksp. No. 2,

7 (1976).
[145]J. B. Natowitz, Phys. Rev. C 1, 623 (1970).
[146]G. N. Flerov, O. Otgonsuren, and V. P. Perelygin, Izv. Akad. Nauk SSSR, Ser. Fiz. 39, 388 (1975).
[147]V. A. Nikolaev *et al.*, Prib. Tekh. Eksp. No. 4, 88 (1976).
[148]J. Aschenbach *et al.*, Nucl. Instrum. Methods 116, 389 (1974).
[149]Alpha-, Beta- and Gamma-Ray Spectroscopy, Vols. 1 and 2 (ed. K. Siegbahn), North-Holland, Amsterdam (1965) (Russian translation published by Atomizdat, Moscow (1969)).

Translated by Julian B. Barbour